Determining 5HT$_7$R's involvement in modifying the antihyperalgesic effects of electroacupuncture on rats with recurrent migraine

Lu Liu（✉ lululalavictor1985@126.com ）
  Capital Medical University   https://orcid.org/0000-0002-7496-5564

Xiaobai Xu
  Beijing Hospital of Traditional Chinese Medicine, Capital Medical University

Zhengyang Qu
  China Academy of Chinese Medical Sciences

Luopeng Zhao
  Beijing Hospital of Traditional Chinese Medicine, Capital Medical University

Claire Shuiqing Zhang
  School of Health and Biomedical Sciences, RMIT University

Zhijuan Li
  Beijing Hospital of Traditional Chinese Medicine, Capital Medical University

Tianli Lyu
  Beijing Hospital of Traditional Chinese Medicine, Capital Medical University

Xuefei Wang
  Beijing Hospital of Traditional Chinese Medicine, Capital Medical University

Xianghong Jing
  Beijing Hospital of Traditional Chinese Medicine

Bin Li
  Beijing Hospital of Traditional Chinese Medicine

Abstract

Background: Electroacupuncture (EA) is widely used in clinical practice to relieve migraine pain. 5-HT$_7$ receptor (5-HT$_7$R) has been reported to play an excitatory role in neuronal systems and regulate hyperalgesic pain and neurogenic inflammation. 5-HT$_7$R could influence Phosphorylation of protein kinase A (PKA)- or Extracellular signal-regulated kinase$_{1/2}$ (ERK$_{1/2}$)-mediated signaling pathways, which mediate sensitization of nociceptive neurons via interacting with cyclic Adenosine monophosphate (cAMP). In this study, we evaluated the role of 5-HT$_7$R in the antihyperalgesic effects of EA and the underlying mechanism through regulation of PKA and ERK$_{1/2}$ in trigeminal ganglion (TG) and trigeminal nucleus caudalis (TNC).

Methods: Hyperalgesia was induced in rats with dural injection of inflammatory soup (IS) to cause meningeal neurogenic inflammatory pain. Electroacupuncture was applied for 15 minutes every other day before IS injection. Von Frey filaments, tail-flick, hot-plate, and cold-plated tests were used to evaluate the mechanical and thermal hyperalgesia. Neuronal hyperexcitability in TNC was studied by an electrophysiological technique. The 5-HT$_7$R antagonist (SB269970) or 5-HT$_7$R agonist (AS19) was administered intrathecally before each IS application at 2-days intervals during the 7-days injection protocol. The changes in 5-HT$_7$R and 5-HT$_7$R-mediated signaling pathway were examined by real time polymerase chain reaction (RT-PCR), Western blot, immunofluorescence and enzyme-linked immunosorbent assay (ELISA) analyses.

Results: When compared with IS group, mechanical and thermal pain thresholds of the IS+EA group were significantly increased. Furthermore, EA prevented the enhancement of both spontaneous activity and evoked responses of second-order trigeminovascular neurons in TNC. Remarkable decreases in 5-HT$_7$R mRNA expression and protein levels were detected in the IS+EA group. More importantly, 5-HT$_7$R agonist AS19 impaired the antihyperalgesic effects of EA on p-PKA and p-ERK$_{1/2}$. Injecting 5-HT$_7$R antagonist SB-269970 into the intrathecal space of IS rats mimicked the effects of EA antihyperalgesia and inhibited p-PKA and p-ERK$_{1/2}$.

Conclusion: Our findings indicate that 5-HT$_7$R mediates the antihyperalgesic effects of EA on IS-induced migraine pain by regulating PKA and ERK$_{1/2}$ in TG and TNC.

Introduction

The pain associated with migraine is a major cause of its accompanying disability and can impact almost every aspect of daily living[1, 2]. A widely-accepted mechanism posits that migraine pain is caused by activation of the trigeminovascular system[3-5], which involves algogenic and inflammatory substances such as nitric oxide, Calcitonin gene-related peptide (CGRP), neurokinin A, substance P, prostaglandins, and cytokines in the meninges, where by their release would influence the activation of trigeminovascular afferents[6-9]. These substances can alter the trigeminal nociceptor excitability

through transcriptional and/or posttranslational mechanisms, giving rise to trigeminal ganglion (TG) and trigeminal nucleus caudalis (TNC) neuronal hyperexcitability. Dural application of inflammatory substances, such as capsaicin[10], cytokines[11], complete Freund adjuvant[12], or inflammatory soup (IS)[13] is used to develop meningeal neurogenic inflammatory pain models in rodents. Injection of inflammatory substances promotes phosphorylation of protein kinase A (PKA) and extracellular signal-regulated kinase$_{1/2}$ (ERK$_{1/2}$), which leads to the nuclear translocation and activation of Cyclic Adenosine monophosphate (cAMP) responsive element-binding protein (CREB) by phosphorylation at Ser133[14-16]. An increase in p-CREB allows for more transcriptional regulation of neuronal activation marker *c-Fos* resulting in the maintenance of facilitated trigeminovascular pain transmission.

Electroacupuncture (EA) is one of the typical treatments of traditional Chinese medicine, and it is widely used in clinical practice to relieve migraine pain[17-20]. p-PKA and p-ERK are considered to be the key to activate nociceptive neurons, and maintain peripheral and central sensitization[10, 21, 22]. Our previous investigation found EA shows a direct effect on nociceptive neurons[23, 24]. In addition, several studies[25-27] suggested PKA and ERK$_{1/2}$ in the spinal dorsal horn might involve EA antihyperalgesia. However, the participation of PKA and ERK$_{1/2}$ in EA antihyperalgesia are not been well defined.

5-hydroxytryptamine (5-HT)$_7$ receptor (5-HT$_7$R), belonging to the G protein-coupled receptor superfamily, is one of the most recently discovered members of the serotonin receptor family. Further studies showed that 5-HT$_7$R is associated with mood disorder[28], epilepsy[29], autism spectrum disorder[30], nociception[31] and migraine [32]. 5-HT$_7$R are abundantly expressed in the central and peripheral nervous system, mainly in the thalamus[33], hypothalamus[34], hippocampus, cerebral cortex[35], amygdala[36], cerebellum[37], TNC [38] and TG[39], and have been reported to play an excitatory role in neuronal systems and regulate hyperalgesic pain and neurogenic inflammation[40, 41]. 5-HT$_7$R couples positively to adenylate cyclase (AC) through activating Gαs (the stimulatory Gs protein), resulting in an increase in cAMP[42, 43]. Recent studies showed that 5-HT$_7$R could influence PKA- or ERK$_{1/2}$-mediated signaling pathways, which mediate sensitization of nociceptive neurons via interacting with Gαs-cAMP[44, 45]. Previous studies found that blockade of 5-HT$_7$R mediated craniovascular vasodilatation and perivascular trigeminal nerve endings in migraine rats. Furthermore, the 5-HT$_7$R antagonist SB-269970 reduced neurogenic dural vasodilation[32] and CGRP release[46], a key neuropeptide in the pathophysiology of migraine.

Given that EA could prevent the phosphorylation of PKA and ERK$_{1/2}$, while the activation of 5-HT$_7$R could cause PKA and ERK$_{1/2}$ phosphorylation levels to increase, we hypothesized that 5-HT$_7$R mediates the antihyperalgesic effects of EA by regulating PKA and ERK$_{1/2}$ through Gαs-cAMP signaling.

Materials And Methods

Animals

Male Sprague-Dawley rats weighing 210-260 g (National Institutes for Food and Drug Control, Beijing, China, Certificate number: SYXK 2014-0013) were housed at 20-26 °C in plastic cages (size: 461 x 274 x 229 mm; 3-4 rats per cage) on soft bedding with ad libitum water and food under a 12h/12h light/dark cycle for at least one week before the experiment. Every effort was made to minimize the number of animals used. Numbers of animals were selected according to previous experience, i.e. a trade-off between reaching routine sample sizes for field experiments while minimizing numbers of animals for pain experiments. Experiments were performed on 100 animals (5-10 rats/group). Rats were randomized into treatment groups before their assessment. All experiments, analysis and reporting were ARRIVE-compliant (Animals in research: reporting in vivo experiments). Animal experiments were performed according to the ethical guidelines set by the International Association for the Study of Pain[47]. The protocols applied here for animal care and use were approved by the Animal Experimentation Ethics Committee of Beijing Institute of Traditional Chinese Medicine (Approval number: 2018080102).

Dural cannulation and inflammatory soup injection

The protocols used for the dural cannulation were similar to those described previously[13, 23]. A previous study found that the effects of inflammatory soup (IS) application on the dura were due to the activation of trigeminal afferents and not to a systemic [48]. Rats were briefly anesthetized with sodium pentobarbital (40 mg/kg, ip). The dura of rats was exposed through a 1 mm hole (1 mm left of midline, 1 mm anterior to bregma) and a guide cannula, extending 0.5 mm from the skull surface to avoid irritation of the dural tissue, was inserted into the hole and secured into place with dental acrylic (**see Additional file: Figure S1A**). One week post-surgery, injections (20 μL, 1μL/minute) of IS or artificial cerebrospinal fluid (aCSF) were performed under brief anesthesia (isoflurane, 3% induction, 1.5% maintenance) through the cannula at 2-days intervals during the 7-days injection protocol[13, 49] (**see Additional file: Figure S1B**). Twenty microliters of aCSF were injected as in rats which form the control (Con) group. After recovery, rats were gently placed into the glass chamber for behavioral testing. IS was formulated with histamine, serotonin and bradykinin, all at 2 mM, and prostaglandin E2 (PGE2), at 0.2 mM, respectively, in 10 mM HEPES buffer at pH 5.0, and aCSF contained124 mM NaCl, 2.5 mM KCl, 1.2 mM NaH2PO4, 1.0 mM MgCl2, 2.0 mM CaCl2, 25 mM NaHCO3 and 10 mM glucose.

Direct transcutaneous intrathecal injection

Intrathecal injection was performed as described previously[50]. One week after dural cannulation, rats received direct transcutaneous intrathecal injection before each IS application at 2-days intervals during the 7-days injection protocol. Under isoflurane induced anesthesia (3% induction, 1.5% maintenance), a 25-G needle connected to a 25-μl Hamilton syringe was inserted percutaneously into the vertebral canal between L5 and L6. A tail-flick reaction denoted a successful puncture. A rat was injected intrathecally with 20 μl of 1% Chicago sky blue (C8678, Sigma-Aldrich, USA) to determine whether the drug injected intrathecally was able to reach the L6-S1 spinal cord level. After that, SB269970 (5-HT$_7$R antagonist, 7μL, 5mM dissolved in distilled water; Sigma-Aldrich, USA) or AS-19 (5-HT$_7$R agonist, 15μL, 10μM dissolved in

saline; Sigma-Aldrich, USA) was administered intrathecally with an injection rate of 1µL/minute [51, 52]. Rats that exhibit signs of motor impairment are excluded from the experiment.

Electroacupuncture

Rats in GB20+GB34, GB20+SJ17, GB34+ST36, IS+EA, and IS+AS19+EA group received EA stimulation under anesthetization with isoflurane (3% induction, 1.5% maintenance). The Con, IS and IS+SEA group were also anesthetized at the same time. After immobilization, the rats were scrubbed with 75% alcohol disinfectant at the EA sites before EA was being performed by the acupuncturist with acupuncture needles. For the EA stimulation, four needles, each sized at 0.25 × 13 mm (Suzhou Medical Appliance Factory, Suzhou, China) were inserted at a depth of 1.5 mm in the bilateral head and hind leg at acupoints corresponding to Fengchi (GB20), Yifeng (SJ17), Yanglingquan (GB34), Zusanli (ST36) (**see Additional file: Figure S2 and Table S1**), as described previously[53-56]. The needles were connected to HANS LH202H Han's acupoint nerve stimulator (Beijing Hua Wei Industrial Development Co, Beijing, China). Electroacupuncture stimulation (2-15 Hz alternating wave, 1.0 mA) of 15 minutes was initiated before IS injection. This process was repeated every 2 days (**Fig. 1A**). Sham electroacupuncture (SEA) was acupuncture needle insertion into non-acupoints (approximately 10 mm and 15mm above the iliac crest) without electrical stimulation.

Experimental procedures

Experiment I

To find the best treatment protocol, we compared the effects of electroacupuncture at different acupoints, including GB20+GB34, GB20+SJ17, and GB34+ST36, in changing the cutaneous hyperalgesia and 5-HT_7R expression of IS rats. We performed the 50% facial mechanical withdrawal threshold (50%FMWT), 50% paw mechanical withdrawal threshold (50%PMWT), tail-flick latency (TFL), hot-plate latency (HPL), and cold-plate behaviors (CPB)[57] to evaluate the mechanical and thermal hyperalgesia. 5-HT_7R expression in trigeminal ganglion (TG) and trigeminal nucleus caudalis (TNC) were detected by real time polymerase chain reaction (RT-PCR), Western blot, and immunofluorescence analyses. The rats were randomly divided into 6 groups: repeated dural injection of aCSF (Con group), repeated dural injection of IS (IS group), IS with sham EA (IS+SEA group), IS with EA at GB20 and GB34 point (GB20+GB34 group), IS with EA at GB20 and SJ17 point (GB20+SJ17 group), and IS with EA at GB34 and ST36 point (GB34+ST36 group) group. (n = 10 per group).

Experiment II

To observe the therapeutic effects of electroacupuncture, we examined whether EA can alleviate cutaneous hyperalgesia and neuronal hyperexcitability in TNC, which induced by repeated dural injection of IS, using behavioral testing and electrophysiological recordings. The rats were assigned at random to Con group, IS group, IS+SEA group, IS+EA (best treatment protocol from experiment I) group (n = 10 per group).

Experiment Ⅲ

To investigate whether electroacupuncture affects $5\text{-}HT_7R$-mediated PKA and $ERK_{1/2}$ phosphorylation signaling pathway, we examined $5\text{-}HT_7R$, cAMP production, the total amount of PKA, $ERK_{1/2}$ and CREB, phosphorylation of PKA, $ERK_{1/2}$, CREB, and c-Fos expression by RT-PCR, Western blot, immunofluorescence and enzyme-linked immunosorbent assay (ELISA) analyses in TG and TNC. The animal groups in experiment III were the same as those in experiment II (n = 5 per group).

Experiment Ⅳ

To determine whether $5\text{-}HT_7R$-mediated PKA and $ERK_{1/2}$ phosphorylation signaling pathways are involved in EA's therapeutic effects, we tested cutaneous hyperalgesia, neuronal hyperexcitability in TNC, and $5\text{-}HT_7R$ related protein using behavioral testing, electrophysiological recordings, Western blot and ELISA analyses. The rats were randomly divided into 4 groups: IS group, IS+SB269970 group (IS with $5\text{-}HT_7R$ antagonist SB269970), IS+AS19+EA group (IS+EA with $5\text{-}HT_7R$ agonist AS19), IS+EA group (n = 5 per group).

Behavioral testing

Before their behavioral testing, the rats were acclimatized to the experiment's environment by being exposed to it for 30 minutes a day for two days, and those with an abnormal baseline were excluded. To avoid experimenter bias, the investigator who conducted the behavioral study did not know the type of treatment applied to the rats. On each of the testing days, rats were brought into the testing room for 30 minutes to acclimate them to the environment. As the rats were acclimated to the environment, they did not show signs of anxiety such as defecation or urination), nor did they attempt to escape by climbing onto the plastic cylinder or cage. After the determination of the baseline response (day 0), all behavioral testing was assessed on days 1, 3, 5, 7 after 1 hours of IS injection, and day 8 without IS injection.

Mechanical Withdrawal Threshold (MWT)

Von Frey filaments (Stoelting, Wood Dale, IL) were used to measure the 50% withdrawal threshold using the up-and-down method reported by Dixon[58] and Chaplan[59]. Tests were conducted during the day portion of the circadian cycle only (06:00-18:00 h). For 50% facial mechanical withdrawal threshold (50%FMWT) testing, the rats were placed in a plastic cylinder with two rectangle open windows which allowed full access to the bilateral face. For 50% paw mechanical withdrawal threshold (50%PMWT) testing, the rats were placed in a plastic cylinder with a wire mesh bottom that allowed for full access to the bilateral paws. Behavioral accommodation was allowed for approximately 15 minutes, until cage exploration and major grooming activities ceased. The areas tested were face and mid-plantar hind paw. The face and paw were touched with one of a series of 10 von Frey filaments with logarithmically incremental stiffness (0.4, 0.6, 1, 2, 4, 6, 8, 15, 26 and 60 g). A series of filaments, starting with one that had a buckling weight of 2 g, was applied in a consecutive sequence on the bilateral facial and hind paw with a pressure causing the filament to buckle and held for approximately 6-8 seconds.

The von Frey filaments were presented perpendicular to the facial and plantar surface with sufficient force to cause slight buckling against the bilateral face and paw. Stimuli were presented at intervals of 10 seconds, allowing for apparent resolution of any behavioral responses to previous stimuli. A positive response was noted if the face and paw were sharply withdrawn. Based on previous studies, the cut-off of a 60-gram filament was selected as the upper limit for testing, since stiffer filaments tended to move the entire face or limb rather than to buckle, substantially changing the nature of the stimulus.

According to Dixon[58], optimal threshold calculation by this method requires 6 responses in the immediate vicinity of the 50% threshold. Since the threshold is not known, strings of similar responses may be generated as the threshold is approached from either direction. Accordingly, although all responses were noted, counting of the critical 6 data points did not begin until the response threshold was first crossed, at which time the 2 responses straddling the threshold were retrospectively designated as the first 2 responses of the series of 6. Four additional responses to the continued presence of stimuli that were varied sequentially up or down, based on the rat's response, constituted the remainder of the series [60].

Tail-flick Latency (TFL)

The tail-flick test was used to assess thermal hyperalgesia in the rats. The rats were placed in a plastic cylinder from which its tail protruded. The presence of tail flicking was considered as withdrawal latency. The intensity of the light from the thermal stimulator (IITC Inc., Woodland Hills, CA) was adjusted at the start of the experiment such that average baseline latencies were approximately 3 to 4 seconds, and a cutoff latency of 16 seconds was established. The heat was directed to the distal tail (20 mm from the tip). Three trials were done at intervals of 5 minutes, and the latency (seconds) was the average of 3 trials[61].

Hot-plate Latency (HPL)

The hot-plate test was used to assess thermal hyperalgesia in the rats. The rats were placed on a heated (50 ± 1°C) surface one at a time. Paw licking or jumping was considered as withdrawal latency. A cutoff latency of 50 seconds was established. Three trials were done at intervals of 20 minutes, and the latency (seconds) was the average of 3 trials [62, 63].

Cold Plate Behaviors (CPB)

The cold-plate test was used to assess thermal hyperalgesia in rats. The plate was cooled down to 4 ± 1 °C. Rats were then placed on the plate for 5 minutes and scored. Rats that were walking freely on the 4 °C cold plate for 5 minutes did not exhibit any signs of skin injury, given that this was a mild nociceptive stimulus. The number of paw lifts quantified the response to cold during an observation period of 5 minutes. Three trials were done at intervals of 10 minutes, and the cold plate behaviors (times) was the average of 3 trials[64, 65].

Electrophysiological recordings in the trigeminal nucleus caudalis

Animal preparation

The last IS injection occurred on day 7 and electrophysiological recordings were performed at 2 hours post-injection. As previously described, rats were anesthetized with isoflurane (3% induction, 1.5% maintenance) mixed with oxygen. After the trachea was cannulated and the carotid artery and external jugular vein catheterized, rats were paralyzed by intravenous perfusion of vecuronium bromide (2.4 mg/h) and artificially ventilated with a volume-controlled pump (54-55 strokes/minute). Levels of isoflurane, O2, N2 and end-tidal CO_2 (3.5-4.5%) were measured by an anesthetic gas analyzer (Drager Vamos) during the entire experimental period. The mean arterial blood pressure was continuously monitored (90 to 110 mmHg). The colorectal temperature was kept constant at 38 ± 0.5°C. The eyes of the rat were protected with erythromycin ointment.

The rats were placed in a stereotaxic frame with the head fixed in a ventro-flexed position. The TNC was exposed by removing the overlying musculature, atlanto-occipital membrane, dura mater and a cervical laminectomy, and then flooded with aCSF. The tungsten recording electrode with a diameter of 75 μm, tip diameter of 3-4 μm, and an impedance of 10-15 kΩ (TM33CCINS, World Precision Instruments Shanghai Trading Co., Ltd. China) was carefully implanted into a depth of 0.5-1.5 mm using a microelectrode manipulator (SR-1N, NARISHIGE Co., Ltd. Japan) (**Fig.2A**).

Electrophysiological Recording

Single-unit activities were sampled and analyzed at 100 Hz-50 kHz and were amplified 1k times and displayed on oscilloscopes. The activities went into a window discriminator connected to a CED 1401plus interface (Cambridge Electronic Design) and a computer (Spike 2 version 7.03a software, CED, Cambridge, UK), which allowed sampling and analysis of the spontaneous and evoked neuronal activity. Wide-dynamic range (WDR) neurons were recognized based on their responses to mechanical non-noxious (brushing with a soft brush) and noxious (pinch with forceps) stimulations of their receptive fields as previously described. Specifically, each neuron that responded in a graded manner with increasing firing rates to the stimulus range from non-noxious to noxious intensity was classified as a WDR cell (**see Additional file: Figure S3**). Once a neuron was identified, electrical square-wave stimuli (1.5ms duration) were applied through a pair of stainless-steel needle electrodes subcutaneously placed into the center of the receptive field; the thresholds for eliciting A- and C-fiber-evoked responses were determined. In poststimulus time histograms (PSTHs), A- and C-fiber-evoked responses were distinguished by their latencies, but only C-fiber-evoked responses were considered in the detailed analysis. Previous research showed that burst discharges at latencies ≥ 30ms are elicited by C-fibers[58, 66]. Therefore, all spikes occurring between 30 and 200ms after a stimulus were considered to be C-fiber-evoked. The C-fiber thresholds (Tc) were defined as the stimulation intensities required to evoke neuronal activity with a conductive velocity of 0.4-2 m.s^{-1} [67] . Electrostimulation (ES) of 1Tc (2mA) and 2.5Tc (5mA) were applied to the facial region in this part of the experiment[68]. ES comprising square waves consisted of low-intensity (2mA, 0.75Hz) and high-intensity (5mA, 0.75Hz) stimulation, and ES being applied once for 1.5ms in order, to the most sensitive portion of the cutaneous receptive field. The

responsiveness of electrical stimulation was assessed by recording the responses to 1.5ms application of ES at 2mA and 5mA. Spontaneous activity (spikes.s^{-1} for 60 seconds, 30 minutes after finding the activated neurons for stabilization) was also recorded. Only one cell was tested in each animal, and only cells with spike amplitude more than 3mV showing no change in amplitude or waveform throughout the experimental procedure were considered and sorted.

Immunofluorescence

Tissue processing for immunofluorescence

Upon deep anesthesia by intraperitoneal injection of sodium pentobarbital (150 mg/kg), the rat was perfused transcardially with normal saline followed by 4% paraformaldehyde in PBS for 20 minutes. Brain and trigeminal ganglia were isolated and post-fixed 30 minutes in the same fixative at room temperature. All specimens were dehydrated for cryoprotection in 30% sucrose in 0.1 M phosphate buffer (0.08 M K2HPO4, 0.02 M NaH2PO4, pH 7.4). TG and TNC in random orientation were cut with a cryostat into 20μm sections and mounted directly onto gelatin-coated slides. From 5 TG and TNC sections (100mm apart) in each rat, total 25 sections were selected for measurement in each group.

Single-labeling immunofluorescence

The sections obtained were washed in Tris-buffered saline (TBS, 25 mM Tris, pH 7.5) and then TBS containing 0.3% Triton X-100 (TBST), sections were treated with 0.3% hydrogen peroxide in TBS to exhaust endogenous hydrogen peroxidase activity until no bubbles. Nonspecific binding was blocked by 3% normal serum (from an animal species same as the secondary antibody) and 2% bovine serum albumin in TBST for 1.5 hours. Sections were incubated with primary antibodies goat anti-CGRP (1:100, ab36001, Abcam, Cambridge, UK) in TBST at room temperature overnight containing 5% normal serum. After overnight reaction with the primary antibody, the sections were washed with TBST and then incubated for 1.5 hours with secondary antibodies rabbit anti-goat IgG labeled with FITC (1:200, RAG001, MultiSciences Biotech Co., Ltd, Hangzhou, China).

Double-labeling immunofluorescence

The following procedures were used for two primary antibodies derived from different species. Sections were processed similarly to that described under the section 'Single-antigen immunohistochemistry'. Primary antibodies included rabbit anti-5-HT$_7$R (1:200, ab61562, Abcam, Cambridge, UK), mouse anti-NeuN (1:1000, ab104224, Abcam, Cambridge, UK). Secondary antibodies included goat anti-rabbit IgG labeled with Alexa 488 (1:200, A0432, Beyotime Biotech Inc., Shanghai, China) and goat anti-mouse IgG labeled with Cy3 (1:200, A0432, Beyotime Biotech Inc., Shanghai, China). Sections on slides were dehydrated through an ethanol gradient/xylene and cover-slipped in antifade mounting medium with DAPI (H-1500, Vector Laboratories, Inc., Burlingame, CA). The images were captured using a Leica semi-automatic light microscope (Leica DM5500B), and processed with the Adobe Photoshop CS2 software. The CGRP-, 5-HT$_7$R-, and NeuN- positive fluorescence images were measured in squares at 20 ×

magnification. ImageJ 1.40g (National Institutes of Health, Bethesda, MD) was used as the software to circle the immunoreactive regions on the soma of TG and TNC neurons.

Western blot

ImageJ 1.40g (National Institutes of Health, Bethesda, MD) was used as the software to circle the immunoreactive regions on the soma of TH and TNC neurons. Punches of TNC regions were selected using a magnifying glass with stainless steel cannulae of 1000 μm inner diameter and subsequently pooled. The tissue was homogenized on the ice with the lysis buffer. The supernatant was collected after centrifugation at 4°C for 20 minutes at 12000 rpm. After being heated at 99°C for 5 minutes, the samples (20 μg/sample) were loaded onto a 5% stacking/10% separating SDS-polyacrylamide gel and then electrophoretically transferred onto a PVDF membrane (Millipore, MA). The membranes were incubated first in the blocking buffer (3% nonfat milk plus 0.1% Tween-20 in the Tris-buffered saline) for 2 hours at room temperature and then in the primary antibodies at 4°C overnight. The primary antibodies included: rabbit anti-5-HT$_7$R (1:2000, ab128892, Abcam, Cambridge, UK), mouse anti-c-Fos (1:2000, ab190289, Abcam, Cambridge, UK), rabbit anti-PKA (1:2000, 4782, CST, USA), rabbit anti-p-PKA (1:2000 5661, CST, USA), rabbit anti-ERK$_{1/2}$ (1:2000 , 4695, CST, USA), rabbit anti-p-ERK$_{1/2}$ (1:2000, 4370, CST, USA), rabbit anti-CREB (1:2000, 4820, CST, USA), rabbit anti-p-CREB (1:2000, 9198, CST, USA), mouse anti-β-actin (1:2000, C1313, Applygen Technologies Inc., Beijing, China). After the membranes were incubated with either the horseradish peroxidase-conjugated anti-rabbit or anti-mouse secondary antibody (1:200, 70-GAM007, MultiSciences, Biotech Co., Ltd, Hangzhou, China) at room temperature for 1 hour, the enhanced chemiluminescence reagent (Bio-Rad Laboratories) were used to visualize the proteins. ChemiDoc XRS and System with Image Lab software (Bio-Rad Laboratories) were performed to generate the images. ImageJ 1.40g software (National Institutes of Health, Bethesda, MD) was used to quantify the intensity of the images. The band intensities for 5-HT$_7$R and c-Fos proteins were normalized to β-actin, and those for PKA, ERK$_{1/2}$, CREB phosphorylation proteins were normalized to these total proteins.

Enzyme-linked immunosorbent assay

The endogenous levels of cAMP were measured in TG and TNC using an enzyme immunoassay kit (EXP110254, Expandbio, Beijing, China) according to the manufacturer's instructions. The concentrations of cAMP were expressed as pmol/mg of protein concentrations calculated in these supernatants.

Real time polymerase chain reaction

Total RNA was extracted from TG and TNC with Trizol reagent (Tiangen Biotech Co., Ltd, Beijing, China). cDNA was synthesized using the PrimeScript RT reagent Kit with gDNA Eraser (RR047B, TaKaRa, Dalian, China). RT-PCR was performed in a real-time PCR system (ABI7500; Applied Biosystems, Foster City, CA) using the SYBR Premix Ex Taq II (Tli RNaseH Plus) ROX plus (RR42LR, TaKaRa, Dalian, China). The PCR cycle parameters consist of an initial 30s incubation at 95°C, followed by 40 cycles of 95°C for 5 s, 60°C for 40 s; followed by a melt from 60°C to 99°C. Each primer sequence was as follows: *5-ht7r*. 5'- GGT GAG GCA AAA TGG GAA ATG -3' (forward) and 5'- ACC GCA GTG GAG TAG ATC GTG TAG -3' (reverse); *Gapdh*:

5'- TGG AGT CTA CTG GCG TCT T -3' (forward) and 5'- TGT CAT ATT TCT CGT GGT TCA -3'(reverse). The Ct value of each gene was normalized against that of *Gapdh*. Relative levels of expression were calculated using the comparative ($2^{-\triangle\triangle Ct}$) method.

Statistical analyses

All statistical analyses were performed using SAS version 9.4 software. Statistical differences were determined using one-way analysis of variance for Immunofluorescence, Western blot, ELISA, RT-PCR and, and two-way repeated-measures analysis of variance was applied for the data from the behavioral testing. When four groups were compared for Electrophysiology, a Kruskal-Wallis test was used, and when only two groups were compared, a Mann-Whitney test was used. Data in the text and figures were shown as mean ± SEM. The level of significance was set at $P < 0.05$.

Results

Electroacupuncture significantly relieved the inflammatory soup-induced hyperalgesia

Measurements of 50%FMWT, 50%PMWT, TFL, HPL and CPB were used to examine the extent of mechanical and thermal hyperalgesia induced by repeated IS infusion and the antihyperalgesic effects of EA. For cephalic (facial) mechanical hyperalgesia (50%FMWT), the rats of the IS group developed cutaneous mechanical hyperresponsiveness, which from day 1 to day 8 on the ipsilateral side (IS vs Con 50%FMWT, $P < 0.0001$) (**Fig. 1B**). For extracephalic mechanical (50%PMWT) and thermal hyperalgesia (TFL, HPL, and CPB), on day 5 and day 7, the pain (cutaneous hyperalgesia) thresholds for the rats' given IS were significantly lower than those given aCSF (IS vs Con 50%PMWT ipsilateral side, $P < 0.0001$; TFL, $P < 0.0001$; HPL, $P < 0.0001$; CPB, $P < 0.0001$) (**Figs. 1C and 1E-1G**). On day 8, the pain thresholds were sharply recovered to the baseline level (IS vs Con 50%PMWT ipsilateral side, $P = 0.1395$; TFL, $P = 0.2487$; HPL, $P = 0.3931$; CPB, $P = 0.6602$) (**Figs. 1C and 1E-1G**). This is an interesting result of the study that we will discuss later. The above effects were also observed on the contralateral side (IS vs Con 50%FMWT, $P < 0.001$; 50%PMWT, $P < 0.001$) (**Figs. 1B and 1C**).

We compared the effects of electroacupuncture at different acupoints, including GB20+GB34, GB20+SJ17, and GB34+ST36 (**see Additional file: Figures S4A-S4G**), in changing the mechanical and thermal hyperalgesia of IS rats to select the best treatment protocol. We found that EA at GB20+GB34, GB20+SJ17, or GB34+ST36 reduced the cutaneous hyperalgesia. The GB20+GB34 group showed the best effect that reduced cephalic mechanical (GB20+GB34 vs IS 50%FMWT ipsilateral side, $P = 0.0003$, 50%FMWT contralateral side, $P < 0.0001$) (**see Additional file: Figures S4A and S4B**), extracephalic mechanical (GB20+GB34 vs IS 50%PMWT ipsilateral side, $P = 0.0009$; 50%PMWT contralateral side, $P = 0.0003$) (**see Additional file: Figures S4C and S4D**), and extracephalic thermal hyperalgesia (GB20+GB34 vs IS TFL, $P = 0.002$; HPL, $P < 0.0001$; CPB, $P = 0.0005$) (**see Additional file: Figures S4E-S4G**) respectively. The following experiments were all performed at GB20+GB34.

EA treatment at GB20+GB34 have shown to reliably inhibit the IS-induced decrease in 50%FMWT on day 1 (ipsilateral side, P = 0.0015; contralateral side, P = 0.0006), day 3 (ipsilateral side, P < 0.0001; contralateral side, P = 0.0002), day 5 (ipsilateral side, P < 0.0001; contralateral side, P < 0.0001), day 7(ipsilateral side, P = 0.0001; contralateral side, P < 0.0001) and day 8 (ipsilateral side, P < 0.0001; contralateral side, P < 0.0001) (**Figs. 1B and 1C**) , and blocked the IS-induced reduction in 50%PMWT on day 7 (ipsilateral side, P = 0.0004; contralateral side, P = 0.0001) (**Figs. 1D and 1E**) on both the ipsilateral and contralateral sides. Furthermore, EA significantly decreased the thermal hypersensitivity on day 5 (IS+EA vs IS TFL, P = 0.0002; HPL, P < 0.0001; CPB, P = 0.0189) and day 7 (IS+EA vs IS TFL, P = 0.001; HPL, P < 0.0001; CPB, P = 0.0002) (**Figs. 1F-1H**). There was no significant difference between the IS+SEA group and the IS group in mechanical (50%FMWT ipsilateral side, P = 0.1155, contralateral side P = 0.8548; 50%PMWT ipsilateral side, P = 0.2632, contralateral side P = 0.1286) (**Figs. 1B-1E**) and thermal hyperalgesia (TFL, P = 0.3858; HPL, P = 0.0859; CPB, P = 0.9555) (**Figs. 1F-1H**). These results indicated that EA could relieve the IS-induced mechanical and thermal hyperalgesia.

The fluorescence intensity of CGRP in the Con and IS group was also tested (**see Additional file: Figures S5A-S5D**). Compared with Con group, the expression of CGRP in IS increased by about 31% and 22.5 % in TG (P = 0.0008) and TNC (P = 0.0008), respectively. Based on the changes in the pain threshold and the detection of CGRP in IS rats, the construction of our recurrent migraine model was successful.

Electroacupuncture prevented neuronal sensitization in TNC

As previously studied, repeated IS-induced persistent sensitization also manifests as enduring enlargement of receptive fields, increases in spontaneous activity, enhancement of Von Frey filament-evoked responses and reduction in mechanical thresholds[48]. Using electrophysiological recordings, we tested whether EA treatment can prevent such persistent neuronal changes.

24 trigeminovascular WDR neurons (1 neuron/animal) receiving convergent input from the dura and facial (cephalic) skin, within the TNC of Con (n = 6), IS rats (i.e. that had already received 4 IS injections; that is at 2 hours after 4th IS injections; n = 6), sham EA- (n = 6) and EA-treated rats (n = 6) were recorded. When tested before anesthesia, sham EA treated, but not EA-treated, rats exhibited a cephalic (facial region) and extracephalic (hindpaw) mechanical and thermal hyperalgesia (mechanical hyperalgesia: 50%FMWT ipsilateral side 1.444 ± 0.2497g and 8.924 ± 0.9632g, P = 0.0009, contralateral side 1.466 ± 0.5094g and 7.318 ± 0.6177g, P = 0.0009 in sham EA- and EA-treated rats, respectively; 50%PMWT ipsilateral side 9.864 ± 1.15g and 16.23 ± 3.414g, P = 0.0015, contralateral side 13.81 ± 1.297g and 19.62 ± 0.4066g, P = 0.0008 in sham EA- and EA-treated rats, respectively; thermal hyperalgesia: HPL 7.604 ± 0.6489s and 11.26 ± 0.3213s, P = 0.0225 in sham EA- and EA-treated rats, respectively; CPB 3 ± 0.2166 times and 1.633 ± 0.2556 times, P = 0.0576 in sham EA- and EA-treated rats, respectively; TFL 2.082 ± 0.07458s and 2.828 ± 0.08946s, P = 0.0038 in sham EA- and EA-treated rats, respectively). Recorded neurons were all located within the deep laminae (IV-VI) of TNC (**Fig. 2B**). When percutaneous electrical stimuli were applied to the center of the cutaneous receptive field of these WDR neurons, responses attributable to peripheral activation of C fibers could be observed for all recorded neurons. Mean latencies

of C-fiber-evoked responses were 52.33 ± 6.302 ms in Con rats, and 49.67 ± 5.76 ms in IS rats(**Fig. 2D**). Computed conduction velocities (~0.4-0.5 m.s^{-1}) were in the range of those previously reported for C fibers[67, 69].

Neurons in rats from the Con group exhibited little or no spontaneous activity (1.35 ± 0.2299 spikes.s^{-1}, **Figs. 2C and 2E**). Low-intensity electrostimulation (LES)-evoked responses, 5.833 ± 0.8333 spikes.s^{-1} (**Figs. 2F and 2H**), and high-intensity electrostimulation (HES)-evoked responses, 9.167 ± 1.537 spikes.s^{-1}(**Figs. 2G and 2H**). Compared with neurons in Con rats, neurons in 4th IS rats presented stronger spontaneous activity (9.267 ± 0.5204 spikes.s^{-1}, P = 0.003948; **Figs. 2C and 2E**), LES-evoked responses (16.67 ± 2.108 spikes.s^{-1}, P = 0.003353; **Figs. 2F and 2I**), and HES-evoked responses (26.67 ± 2.108 spikes.s^{-1}, P = 0.003403; **Figs. 2G and 2I**). These results indicate that trigeminovascular WDR neurons become sensitized following repeated activation of dural nociceptors.

In sham EA-treated rats, neurons exhibited high spontaneous activity (8.542 ± 0.5463 spikes.s^{-1}; **Figs. 2C and 2E**), and large LES- and HES- evoked responses (15.83 ± 2.386 spikes.s^{-1} and 25 ± 2.582 spikes.s^{-1}, respectively; **Figs. 2F-2G and 2J**). This suggests that the responses of WDR neurons to electrical stimulations were not changed after repeated sham-EA. On the other hand, compared with sham EA-treated rats, WDR neurons recorded in EA-treated rats exhibited lower spontaneous activities (3.008 ± 0.3957 spikes.s^{-1}, P = 0.003948; **Fig. 2E**), smaller LES- (9.167 ± 1.537 spikes.s^{-1}, P = 0.044277; **Fig. 2F**) and HES-evoked responses (15.83 ± 2.386 spikes.s^{-1}, P = 0.033118; **Fig. 2G**). Thus, EA appears to completely prevent the sensitization of WDR neurons induced by repeated IS injections. Together, these data demonstrate that EA acquired antihyperalgesic properties by decreasing TNC nociceptive activity in response to IS inflammation.

Electroacupuncture significantly reduced the expression of 5-HT$_7$R in TG and TNC

To determine whether the effects of EA were associated with 5-HT$_7$R, we performed RT-PCR, Western blot, and immunofluorescence analyses. Samples for RT-PCR were respectively collected on day 8 after 4th IS injection. There were significant changes in the 5-HT$_7$R mRNA expression in response to IS injection compared with the Con group in TG and TNC (TG, P < 0.0001; TNC, P < 0.0001). However, the 5-HT$_7$R mRNA level of the IS+EA group was significantly reduced compared with that of the IS group in TG and TNC (TG, P < 0.0001; TNC, P < 0.0001) (**Figs. 3D and 4D**). Next, we examined the total protein content of 5-HT$_7$R in Con, IS, IS+SEA, and IS+EA groups by Western blot analysis. Significant differences were observed in both TG and TNC between the IS group and the Con group (TG, P = 0.0165; TNC, P = 0.0007). EA treatment significantly reduced the 5-HT$_7$R protein content compared with the IS group (TG, P = 0.0163; TNC, P = 0.0009) (**Figs. 3C and 4C**). We also used immunofluorescence double labeling to detect the distribution of 5-HT$_7$R in TG and TNC, and found 5-HT$_7$R were colocalized with neurons (**Figs. 3A and 4A, 3th column, orange arrowheads**). IF analysis revealed increased 5-HT$_7$R positive cells were double-positive for NeuN in IS group compared with the Con group, and 5-HT$_7$R proteins were expressed in large-

sized TG neurons in immunostaining of TG sections (**Figs. 4A, 1st column, white arrowheads**). Consistent with the Western blot results, the 5-HT$_7$R level seemed to reduce in the IS+EA group compared with the IS group (TG, P = 0.0003; TNC, P = 0.0037) (**Figs. 3A-3B and 4A-4B**). There were significant differences between the IS+EA and IS+SEA group in the abovementioned test (RT-PCR: TG, P < 0.0001; TNC, P < 0.0001; WB: TG, P = 0.0207; TNC, P = 0.0457; IF: TG, P = 0.0132; TNC, P = 0.0114) (**Figs. 3A-3D and 4A-4D**). These results indicated that EA relieved IS-induced hyperalgesia, which is shown by a reduction in 5-HT$_7$R expression.

The effects of electroacupuncture at different acupoints were also compared, including GB20+GB34, GB20+SJ17, and GB34+ST36 (**see Additional file: Figures S6A-S6E and S7A-S7E**), in changing the 5-HT$_7$R expression of IS rats. We found that EA at GB20+GB34, GB20+SJ17, or GB34+ST36 reduced the 5-HT$_7$R expression. The GB20+GB34 group showed the best effect that reduced 5-HT$_7$R expression.

Electroacupuncture inhibited the 5-HT$_7$R-mediated PKA and ERK$_{1/2}$ phosphorylation signaling pathway in TG and TNC

It is known that 5-HT$_7$R could influence PKA- or ERK$_{1/2}$-mediated signaling pathways through interacting with Gαs-cAMP[44, 45] and the increasing PAK-p and p-ERK$_{1/2}$ could be blocked by EA treatment. As a result, 5-HT$_7$R related protein content of cAMP, PKA, p-PKA, ERK$_{1/2}$, p-ERK$_{1/2}$, CREB and p-CREB were also detected. As we first measured the cAMP levels, a significant difference was shown between EA and IS groups (TG, P < 0.0001; TNC, P < 0.0001) (**Figs. 5A and 5F**), suggesting that EA-induced 5-HT$_7$R inhibition is cAMP-dependent.

Next, we found that the protein expression of p-PKA (TG, P = 0.0003; TNC, P < 0.0001), p-ERK$_{1/2}$ (TG, P < 0.0001; TNC, P < 0.0001), and p-CREB (TG, P < 0.0001; TNC, P < 0.0001) in IS group was increased compared with the Con group, and EA treatment inhibited p-PKA (TG, P = 0.0003; TNC, P < 0.0001), p-ERK$_{1/2}$ (TG, P < 0.0001; TNC, P < 0.0001) and p-CREB (TG, P < 0.0001; TNC, P < 0.0001) expression (**Figs. 5B-5D and 5G-5I**). However, there was no significant difference in total amount of PKA, ERK$_{1/2}$ and CREB between the four groups (**Figs. 5B-5D and 5G-5I**).

C-Fos, that is a classical marker of neuronal activation with trigeminovascular nociceptive pathways[70], could be initiated or potentiated by CREB phosphorylation. Here, we found that, the expression of c-Fos in IS group was increased (TG, P = 0.0022; TNC, P = 0.0056) compared with the Con group. However, the expression of c-Fos was suppressed after EA treatment (TG, P = 0.0022; TNC, P = 0.003) (**Figs. 5E and 5J**). Sham EA had no effect on the expression of cAMP, p-PKA, p-ERK$_{1/2}$, p-CREB and c-Fos (IS+SEA vs IS) (**Figs. 5A-5J**). The above results demonstrated that EA inhibited the 5-HT$_7$R-mediated PKA and ERK$_{1/2}$ phosphorylation signaling pathway in TG and TNC.

Antihyperalgesic effects and inhibition of neuronal sensitization produced by electroacupuncture were weakened in 5-HT$_7$R agonist AS19-treated IS rats, and mimicked in 5-HT$_7$R antagonist SB269970-treated IS rats

Based on our results that EA reduced the content of 5-HT$_7$R, we used a pharmacological strategy to reveal the role of 5-HT$_7$R in the antihyperalgesic effects and inhibition of neuronal sensitization of EA (**Fig. 6A**). To measure the changes in cutaneous hyperalgesia and nociceptive neuron activity, the rats from EA and non-EA groups were injected with either 5-HT$_7$R antagonist (SB269970) or 5-HT$_7$R agonist (AS19) before being injected with IS.

Injection of IS induced a significant decrease of hyperalgesia intensity in SB269970-treated rats on day 7 (IS+SB269970 vs IS mechanical hyperalgesia: 50%FMWT ipsilateral side, P = 0.0046; 50%FMWT contralateral side, P = 0.0210, 50%PMWT ipsilateral side, P = 0.0023; 50%PMWT contralateral side, P = 0.0165; thermal hyperalgesia: TFL P = 0.0013, HPL P = 0.0333, CPB P = 0.0029 (**Figs. 6B-6H**), but such differences were absent in IS+SB269970 and IS+EA rats (IS+SB269970 vs IS+EA mechanical hyperalgesia: 50%FMWT ipsilateral side, P = 0.1047; 50%FMWT contralateral side, P = 0.5108, 50%PMWT ipsilateral side, P = 0.2588; 50%PMWT contralateral side, P = 0.2287; thermal hyperalgesia : TFL P = 0.193, HPL P = 0.5863, CPB P = 0.6699) (**Figs. 6B, 6D and 6F-6H**). Compared with IS rats (**Figs. 7A-7E**), WDR neurons recorded in IS+SB269970 rats exhibited lower spontaneous activities (2.892 ± 0.4142 spikes.s^{-1}, P = 0.003948; **Fig.7B**), smaller LES- (9.167 ± 1.537 spikes.s^{-1}, P = 0.016864; **Figs. 7C and 7F**) and HES-evoked responses (16.67 ± 2.108 spikes.s^{-1}, P = 0.0065; **Figs. 7D and 7F**). The electrophysiological properties of IS+SB269970 rats were similar to those of IS+EA rats (spontaneous activities, P = 0.8728; LES-evoked responses; P = 0.6654; HES-evoked responses P = 0.7370, **Figs.7A-7D and 7H**). Together, these data indicated that SB269970 mimics the antihyperalgesic effects and inhibition of neuronal sensitization of EA.

The hyperalgesia intensity of the IS+AS19+EA group was significantly aggravated when compared against the IS+EA group (IS+AS19+EA vs IS+EA mechanical hyperalgesia: 50%FMWT ipsilateral side, P = 0.0074; 50%FMWT contralateral side, P = 0.0069, 50%PMWT ipsilateral side, P = 0.0124; 50%PMWT contralateral side, P = 0.0002; thermal hyperalgesia: TFL P = 0.0095, HPL P < 0.0001, CPB P = 0.0363), whereas no differences were seen between the IS and IS+AS19+EA groups (**Figs. 6B-6H**). Low spontaneous activities, small LES- and HES-evoked responses in IS+EA rats were activated by AS19 (IS+AS19+EA vs IS+EA spontaneous activities P = 0.0039; LES-evoked responses P = 0.0165; HES-evoked responses P = 0.0049) (**Figs. 7B-7D and 7G-7H**). Together, these data indicated that the antihyperalgesic effects and inhibition of neuronal sensitization produced by EA treatment were weakened in AS19-treated IS rats. The abovementioned finding suggested that 5-HT$_7$R is necessary for EA antihyperalgesia and inhibition of neuronal sensitization.

5-HT$_7$R-mediated PKA and ERK$_{1/2}$ phosphorylation through cAMP signaling may be involved in EA's antihyperalgesic effects

The behavioral analysis showed that the activation of 5-HT$_7$R weakened, but did not completely abolished the relatively reduced intensity of the antihyperalgesic effects of EA. To explore the reason why the antihyperalgesic effects of EA were weakened in the AS19-treated rats, we examined the protein

content of cAMP, PKA, p-PKA, $ERK_{1/2}$, p-$ERK_{1/2}$, CREB and p-CREB, c-Fos, which plays a pivotal role in the 5-HT_7R-mediated transmission of nociceptive information. Electroacupuncture reduced the cAMP, p-PKA, p-$ERK_{1/2}$, p-CREB, c-Fos level to the baseline level in IS rats (IS vs IS+EA) (**Figs. 8A-8J**), which was related to the antihyperalgesic effects confirmed by relevant studies. Electroacupuncture significantly downregulated cAMP, p-PKA, p-$ERK_{1/2}$, p-CREB, c-Fos expression in IS rats but not in AS19-treated IS rats (IS+EA vs IS+AS19+EA, cAMP: TG, $P < 0.0001$; TNC, $P = 0.0029$; p-PKA: TG, $P = 0.0053$; TNC, $P = 0.0364$; p-$ERK_{1/2}$: TG, $P = 0.0006$; TNC, $P = 0.0002$; p-CREB: TG, $P = 0.0024$; TNC, $P = 0.0003$ c-Fos: TG, $P = 0.0005$; TNC, $P = 0.0039$) (**Figs. 8A-8J**).The WB results suggested that 5-HT_7R activation likely weakened the regulation of cAMP, p-PKA, p-$ERK_{1/2}$, p-CREB, and c-Fos by EA, but did not completely inhibit the effect. In addition, EA did not affect the content of PKA, $ERK_{1/2}$ and CREB in both IS and AS19-treated IS rats (**Figs. 8B-8D and 8G-8I**). These results indicate that AS19 impaired the suppression effects of EA on endogenous cAMP, p-PKA, p-$ERK_{1/2}$, p-CREB, c-Fos, which could explain that the antihyperalgesic effects of EA were weakened in the AS19-treated IS rats.

   Then, we detected the effects of the 5-HT_7R antagonist (SB269970) on the above protein levels. It could inhibit cAMP, p-PKA, p-$ERK_{1/2}$, p-CREB expression in TG and TNC of IS rats by injecting 7μL of SB269970 (5mM) into the intrathecal space (cAMP: TG, $P < 0.0001$; TNC, $P = 0.0005$; p-PKA: TG, $P = 0.0059$; TNC, $P = 0.0256$; p-$ERK_{1/2}$: TG, $P = 0.0001$; TNC, $P < 0.0001$; p-CREB: TG, $P = 0.0282$; TNC, $P = 0.0001$) (**Figs. 8A-8D and 8F-8I**). This is consistent with the results that EA decreases the expression of 5-HT_7R-mediated signaling pathways related protein. Then, it inhibited p-CREB-mediated transcriptional regulation factor c-Fos (TG, $P = 0.0006$; TNC, $P = 0.0016$) (**Figs. 8E and 8J**). This mimics the antihyperalgesic effects of EA and inhibited p-PKA, p-$ERK_{1/2}$, p-CREB. There was also no statistical difference in PKA, $ERK_{1/2}$, and CREB (**Figs. 8B-8D and 8G-8I**). Based on the results, we concluded that 5-HT_7R-mediated PKA and $ERK_{1/2}$ phosphorylation signaling pathways may be involved in EA antihyperalgesia.

Discussion

To our knowledge, this study is the first research which demonstrates that EA decreased IS-induced elevated content of 5-HT_7R in the TG and TNC, suggesting that there is certain relationship between 5-HT_7R expression and EA treatment. 5-HT_7R agonist AS19 impaired the antihyperalgesic effects of EA on p-PKA and p-$ERK_{1/2}$. Injecting 5-HT_7R antagonist SB-269970 into the intrathecal space of IS rats mimicked the effects of EA antihyperalgesia and inhibited p-PKA and p-$ERK_{1/2}$, indicating decreased 5-HT_7R expression and decreased p-PKA and p-$ERK_{1/2}$ expression are sufficient to EA treatment.

It is known that 5-HT_7R-mediated PKA and $ERK_{1/2}$ activation is dependent on a Gαs-cAMP signaling in the nervous system, we speculated the potential mechanisms as follows (**Fig. 9**). Upon IS dural injection, 5-HT_7R is stimulated to couple positively with adenylate cyclase (AC) through activating Gαs, resulting in an increase of cAMP to ultimately phosphorylate PKA and $ERK_{1/2}$. Phosphorylation of PKA and $ERK_{1/2}$ causes the nuclear translocation of CREB so that making it activation by phosphorylation at Ser133. The

consequent increase in nuclear CREB-CBP complex in trigeminal ganglion (TG) and trigeminal nucleus caudalis (TNC) might initiate or potentiate p-CREB-mediated transcriptional regulation of immediate early gene *c-fos that is sufficient to neuronal activation with trigeminovascular* nociceptive pathways[70]. On EA treatment, 5-HT$_7$R decreased, leading to a decrease in the content of cAMP so that less formation of p-PKA and p-ERK$_{1/2}$ might be retained in the cytoplasm, which attenuates induced CREB phosphorylation and transcriptional pronociceptive gene **(Fig. 9)**. Ultimately, a series of the abovementioned processes would not occur under EA treatment. Then, the trigeminovascular nociceptive sensitization could be unsustainable. Therefore, our results suggest that 5-HT$_7$R mediates the antihyperalgesic effects of EA and indicates that the Gαs-cAMP signaling may be a new underlying mechanism.

However, how EA regulates 5-HT$_7$R remains unclear. Electroacupuncture was reported to reduce the cytoplasmic content of cAMP[26]. Decreased cAMP affects the phosphorylation of PKA and ERK$_{1/2}$[71, 72]. Given the interaction between Gαs-cAMP and 5-HT$_7$R, the possibility of EA affecting 5-HT$_7$R exists. This specific mechanism would be a direction for our further research. Notably, the antihyperalgesic effects of EA were weakened but not completely obliterated in the activation of 5-HT$_7$R, due to the inhibition of PKA and ERK$_{1/2}$ phosphorylation. Given that EA could influence multiple signaling pathways, including β-endorphins[73], cannabinoid CB2 receptors[74], and adenosine A1 receptor[75], the 5-HT$_7$R-mediated PKA and ERK$_{1/2}$ phosphorylation through Gαs-cAMP signaling is likely only one of the key factors involved in EA's maintenance of antihyperalgesic effects. Moreover, cAMP interacts with several other proteins in addition to PKA and ERK$_{1/2}$, including ROS[76], NF-κB[77], and AKAP[78], which might also be involved in the maintenance of the antihyperalgesic effects by EA. Next, we will use naloxone to block opioid receptors, or DPCPX to block A1 receptors, so as to exclude the effect of other factors on EA antihyperalgesia, and then confirm the role of 5-HT$_7$R.

We found the extracephalic pain thresholds of IS group were sharply recovered to the baseline level on day 8 but there were significantly lower in the IS group compared with the Con group on day 5 and day 7 **(Figs. 1D-1H)**. However, the IS group maintained persistent cephalic static mechanical hyperalgesia from day 1 to day 8 **(Figs. 1B-1C)**. These results were consistent with the previous investigation on the effect of IS to the cephalic and extracephalic cutaneous hyperalgesia. Boyer et al.[48] found that repeated IS injection (4 times IS protocol) developed reversible extracephalic and persistent cephalic hyperalgesia. Specifically, extracephalic pain thresholds decreased 1 hour after 4th IS injection and returned to pre-IS values within 2-3 hours after 4th IS injection. Cephalic pain thresholds before the 4th IS injection were already lower than those in the Con group. Similarly, we found rats developed lower extracephalic pain thresholds after 1 hour of 3rd and 4th IS injection on day 5 and day 7, and returned to the baseline level on day 8 without IS injection. Furthermore, the repeats of IS produced ever stronger and longer cephalic hyperalgesia from day 1 to day 8. Such repetition of IS-induced development of central sensitization and its consequence, cutaneous hyperalgesia, may arise from hyperexcitability that likely develops in trigeminal nociceptive neurons in response to their repetitive activation **(Figs. 2C-2E)**. EA exerted

antihyperalgesic effects, at least in part, via preventing the maintenance of a state of facilitated trigeminovascular transmission within the TNC.

Based on previous experience[25, 79, 80], we also performed sham EA manipulation to ensure the 5-HT$_7$R is specific in EA antihyperalgesia. The results showed that 5-HT$_7$R expression was not decreased in the IS+SEA group (**Figs. 3A-D and 4A-D**), cAMP was not decreased (**Figs. 5A and 6F**) and there was no statistical difference in p-PKA, p-ERK$_{1/2}$, p-CREB, and c-Fos compared with the IS group (**Figs. 5B-E and 5G-J**), indicating that sham EA had no effect on 5-HT$_7$R and related protein, EA was specific.

Previous studies[44, 45] show that the PKA- or ERK$_{1/2}$-mediated signaling pathways are involved in the CFA-or CA induced long-lasting pain hypersensitivity through 5-HT$_7$R. More expression of p-PKA or p-ERK$_{1/2}$ means more excitation of dura-sensitive trigeminal neurons and more sensitization of pain transducing receptors [81] [22]. Indeed, there were significant differences in the expression of p-PKA and p-ERK$_{1/2}$ between the IS+SB269970 group and the IS group, which is consistent to the previous study. We found that 5-HT$_7$R agonist AS19 could recover EA-induced decreased cAMP and inhibited p-PKA/p-ERK$_{1/2}$ in the TG and TNC. 5-HT$_7$R antagonist SB-269970 generated the antihyperalgesic effects on neurogenic inflammation pain induced by IS, which mimics the effects of EA antihyperalgesia. In addition, we found that the expression of cAMP protein increased with the activation of 5-HT$_7$R, which confirmed the interaction between Gαs-cAMP and 5-HT$_7$R. It indicated 5-HT$_7$R as a new target for enhancing the EA antihyperalgesic efficacy in migraine, and the development and application of related drugs could be promoted furthermore.

Based on our findings, the antihyperalgesic effects of EA have been further verified. As it is now established that 5-HT$_7$R affects the phosphorylation of PKA and ERK$_{1/2}$ through Gαs-cAMP, this interaction could be involved in the facilitation of persistent pain and regulation of peripheral/central sensitization, further highlighting the theory that 5-HT$_7$R mediates the antihyperalgesic effects of EA. Further explorations of the functions and roles of 5-HT$_7$R may reveal new insight into the mechanisms underlying migraine.

Conclusion

In summary, our results indicate that 5-HT$_7$R mediates the antihyperalgesic effects of EA on IS-induced neurogenic inflammation pain by regulating PKA and ERK$_{1/2}$ phosphorylation through cAMP. Our study may provide a new target to enhance the EA antihyperalgesic effects in migraine.

Abbreviations

aCSF: Artificial cerebrospinal fluid; AC: adenylate cyclase; Calcitonin gene-related peptide: CGRP; cAMP: Cyclic Adenosine monophosphate; CREB: Cyclic Adenosine monophosphate responsive element-binding protein; Con: Control; CPB: Cold-plate behaviors; EA: Electroacupuncture; ELISA: Enzyme-linked

immunosorbent assay; ERK$_{1/2}$: Extracellular signal-regulated kinase$_{1/2}$; ES: Electrostimulation; 50%FMWT: 50% facial mechanical withdrawal threshold; 5-HT$_7$R: 5-HT$_7$ receptor; HPL: Hot-plate latency; HES: High-intensity electrostimulation; IS: inflammatory soup; LES: Low-intensity electrostimulation; PKA: Phosphorylation of protein kinase A; PGE2: Prostaglandin E2; 50%PMWT: 50% paw mechanical withdrawal threshold; PSTHs: Poststimulus time histograms; RT-PCR: real time polymerase chain reaction; SEA: Sham electroacupuncture; TG: Trigeminal ganglion; TNC: trigeminal nucleus caudalis; TFL: Tail-flick latency; Tc: C-fiber thresholds; WDR: Wide-dynamic range

Declarations

Availability of data and materials

The datasets during and/or analyzed during the current study are available from the corresponding author on reasonable request.

Ethics approval and consent to participate

Not applicable.

Consent for publication

Not applicable.

Competing interests

The authors of the manuscript have no conflict of interest to report.

References

1. Agosti R: **Migraine Burden of Disease: From the Patient's Experience to a Socio-Economic View.** *Headache* 2018, **58 Suppl 1**:17-32.

2. Collaborators GBDH: **Global, regional, and national burden of migraine and tension-type headache, 1990-2016: a systematic analysis for the Global Burden of Disease Study 2016.** *Lancet Neurol* 2018, **17**:954-976.

3. Ashina M, Hansen JM, Do TP, Melo-Carrillo A, Burstein R, Moskowitz MA: **Migraine and the trigeminovascular system-40 years and counting.** *Lancet Neurol* 2019, **18**:795-804.

4. Noseda R, Burstein R: **Migraine pathophysiology: anatomy of the trigeminovascular pathway and associated neurological symptoms, CSD, sensitization and modulation of pain.** *Pain* 2013, **154 Suppl 1**.

5. Akerman S, Romero-Reyes M, Holland PR: **Current and novel insights into the neurophysiology of migraine and its implications for therapeutics.** *Pharmacol Ther* 2017, **172**:151-170.

6. Goadsby PJ, Edvinsson L: **The trigeminovascular system and migraine: studies characterizing cerebrovascular and neuropeptide changes seen in humans and cats.** *Ann Neurol* 1993, **33**:48-56.

7. Gallai V, Sarchielli P, Floridi A, Franceschini M, Codini M, Glioti G, Trequattrini A, Palumbo R: **Vasoactive peptide levels in the plasma of young migraine patients with and without aura assessed both interictally and ictally.** *Cephalalgia* 1995, **15**:384-390.

8. Sarchielli P, Alberti A, Baldi A, Coppola F, Rossi C, Pierguidi L, Floridi A, Calabresi P: **Proinflammatory cytokines, adhesion molecules, and lymphocyte integrin expression in the internal jugular blood of migraine patients without aura assessed ictally.** *Headache* 2006, **46**:200-207.

9. Sarchielli P, Alberti A, Codini M, Floridi A, Gallai V: **Nitric oxide metabolites, prostaglandins and trigeminal vasoactive peptides in internal jugular vein blood during spontaneous migraine attacks.** *Cephalalgia* 2000, **20**:907-918.

10. Iwashita T, Shimizu T, Shibata M, Toriumi H, Ebine T, Funakubo M, Suzuki N: **Activation of extracellular signal-regulated kinase in the trigeminal ganglion following both treatment of the dura mater with capsaicin and cortical spreading depression.** *Neurosci Res* 2013, **77**:110-119.

11. Zhang X, Burstein R, Levy D: **Local action of the proinflammatory cytokines IL-1β and IL-6 on intracranial meningeal nociceptors.** *Cephalalgia* 2012, **32**:66-72.

12. Lukács M, Warfvinge K, Tajti J, Fülöp F, Toldi J, Vécsei L, Edvinsson L: **Topical dura mater application of CFA induces enhanced expression of c-fos and glutamate in rat trigeminal nucleus caudalis: attenuated by KYNA derivate (SZR72).** *J Headache Pain* 2017, **18**:39.

13. Boyer N, Signoret-Genest J, Artola A, Dallel R, Monconduit L: **Propranolol treatment prevents chronic central sensitization induced by repeated dural stimulation.** *Pain* 2017, **158:**2025-2034.

14. Vermeer LM, Gregory E, Winter MK, McCarson KE, Berman NE: **Exposure to bisphenol A exacerbates migraine-like behaviors in a multibehavior model of rat migraine.** *Toxicol Sci* 2014, **137:**416-427.

15. Ramachandran R, Pedersen SH, Amrutkar DV, Petersen S, Jacobsen JM, Hay-Schmidt A, Olesen J, Jansen-Olesen I: **Selective cephalic upregulation of p-ERK, CamKII and p-CREB in response to glyceryl trinitrate infusion.** *Cephalalgia* 2018, **38:**1057-1070.

16. Levy D, Strassman AM: **Distinct sensitizing effects of the cAMP-PKA second messenger cascade on rat dural mechanonociceptors.** *J Physiol* 2002, **538:**483-493.

17. Zhao L, Chen J, Li Y, Sun X, Chang X, Zheng H, Gong B, Huang Y, Yang M, Wu X, et al: **The Long-term Effect of Acupuncture for Migraine Prophylaxis: A Randomized Clinical Trial.** *JAMA Intern Med* 2017, **177:**508-515.

18. Yang M, Yang J, Zeng F, Liu P, Lai Z, Deng S, Fang L, Song W, Xie H, Liang F: **Electroacupuncture stimulation at sub-specific acupoint and non-acupoint induced distinct brain glucose metabolism change in migraineurs: a PET-CT study.** *J Transl Med* 2014, **12:**351.

19. Li Y, Zheng H, Witt CM, Roll S, Yu SG, Yan J, Sun GJ, Zhao L, Huang WJ, Chang XR, et al: **Acupuncture for migraine prophylaxis: a randomized controlled trial.** *CMAJ* 2012, **184:**401-410.

20. Linde K, Allais G, Brinkhaus B, Fei Y, Mehring M, Vertosick EA, Vickers A, White AR: **Acupuncture for the prevention of episodic migraine.** *Cochrane Database Syst Rev* 2016, **2016:**CD001218.

21. Nakaya Y, Tsuboi Y, Okada-Ogawa A, Shinoda M, Kubo A, Chen JY, Noma N, Batbold D, Imamura Y, Sessle BJ, Iwata K: **ERK-GluR1 phosphorylation in trigeminal spinal subnucleus caudalis neurons is involved in pain associated with dry tongue.** *Mol Pain* 2016, **12**.

22. Giniatullin R, Nistri A, Fabbretti E: **Molecular mechanisms of sensitization of pain-transducing P2X3 receptors by the migraine mediators CGRP and NGF.** *Mol Neurobiol* 2008, **37:**83-90.

23. Qu Z, Liu L, Yang Y, Zhao L, Xu X, Li Z, Zhu Y, Jing X, Wang X, Zhang CS, et al: **Electro-acupuncture inhibits C-fiber-evoked WDR neuronal activity of the trigeminocervical complex: Neurophysiological hypothesis of a complementary therapy for acute migraine modeled rats.** *Brain Res* 2020, **1730:**146670.

24. Qu Z, Liu L, Zhao L, Xu X, Li Z, Zhu Y, Zhang C, Jing X, Wang X, Li B, et al: **Prophylactic Electroacupuncture on the Upper Cervical Segments Decreases Neuronal Discharges of the Trigeminocervical Complex in Migraine-Affected Rats: An in vivo Extracellular Electrophysiological Experiment.** *J Pain Res* 2020, **13:**25-37.

25. Hu Q, Zheng X, Li X, Liu B, Yin C, Li Y, Chen R, Wang J, Liang Y, Shao X, et al: **Electroacupuncture Alleviates Mechanical Allodynia in a Rat Model of Complex Regional Pain Syndrome Type-I via Suppressing Spinal CXCL12/CXCR4 Signaling.** *J Pain* 2020.

26. Shao XM, Sun J, Jiang YL, Liu BY, Shen Z, Fang F, Du JY, Wu YY, Wang JL, Fang JQ: **Inhibition of the cAMP/PKA/CREB Pathway Contributes to the Analgesic Effects of Electroacupuncture in the Anterior Cingulate Cortex in a Rat Pain Memory Model.** *Neural Plast* 2016, **2016:**5320641.

27. Han P, Liu S, Zhang M, Zhao J, Wang Y, Wu G, Mi W: **Inhibition of Spinal Interlukin-33/ST2 Signaling and Downstream ERK and JNK Pathways in Electroacupuncture Analgesia in Formalin Mice.** *PLoS One* 2015, **10:**e0129576.

28. Sarkisyan G, Roberts AJ, Hedlund PB: **The 5-HT(7) receptor as a mediator and modulator of antidepressant-like behavior.** *Behav Brain Res* 2010, **209:**99-108.

29. Yang Z, Liu X, Yin Y, Sun S, Deng X: **Involvement of 5-HT⬚ receptors in the pathogenesis of temporal lobe epilepsy.** *Eur J Pharmacol* 2012, **685:**52-58.

30. Ciranna L, Catania MV: **5-HT7 receptors as modulators of neuronal excitability, synaptic transmission and plasticity: physiological role and possible implications in autism spectrum disorders.** *Front Cell Neurosci* 2014, **8:**250.

31. Brenchat A, Nadal X, Romero L, Ovalle S, Muro A, Sánchez-Arroyos R, Portillo-Salido E, Pujol M, Montero A, Codony X, et al: **Pharmacological activation of 5-HT7 receptors reduces nerve injury-induced mechanical and thermal hypersensitivity.** *Pain* 2010, **149:**483-494.

32. Wang X, Fang Y, Liang J, Yan M, Hu R, Pan X: **5-HT7 receptors are involved in neurogenic dural vasodilatation in an experimental model of migraine.** *J Mol Neurosci* 2014, **54:**164-170.

33. Varnäs K, Thomas DR, Tupala E, Tiihonen J, Hall H: **Distribution of 5-HT7 receptors in the human brain: a preliminary autoradiographic study using [3H]SB-269970.** *Neurosci Lett* 2004, **367:**313-316.

34. Bonaventure P, Nepomuceno D, Hein L, Sutcliffe JG, Lovenberg T, Hedlund PB: **Radioligand binding analysis of knockout mice reveals 5-hydroxytryptamine(7) receptor distribution and uncovers 8-hydroxy-2-(di-n-propylamino)tetralin interaction with alpha(2) adrenergic receptors.** *Neuroscience* 2004, **124:**901-911.

35. Neumaier JF, Sexton TJ, Yracheta J, Diaz AM, Brownfield M: **Localization of 5-HT(7) receptors in rat brain by immunocytochemistry, in situ hybridization, and agonist stimulated cFos expression.** *J Chem Neuroanat* 2001, **21:**63-73.

36. Muneoka KT, Takigawa M: **5-Hydroxytryptamine7 (5-HT7) receptor immunoreactivity-positive 'stigmoid body'-like structure in developing rat brains.** *Int J Dev Neurosci* 2003, **21:**133-143.

37. Geurts FJ, De Schutter E, Timmermans JP: **Localization of 5-HT2A, 5-HT3, 5-HT5A and 5-HT7 receptor-like immunoreactivity in the rat cerebellum.** *J Chem Neuroanat* 2002, **24:**65-74.

38. Martínez-García E, Leopoldo M, Lacivita E, Terrón JA: **Increase of capsaicin-induced trigeminal Fos-like immunoreactivity by 5-HT(7) receptors.** *Headache* 2011, **51:**1511-1519.

39. Terrón JA, Bouchelet I, Hamel E: **5-HT7 receptor mRNA expression in human trigeminal ganglia.** *Neurosci Lett* 2001, **302:**9-12.

40. Bravo L, Llorca-Torralba M, Berrocoso E, Micó JA: **Monoamines as Drug Targets in Chronic Pain: Focusing on Neuropathic Pain.** *Front Neurosci* 2019, **13:**1268.

41. Terrón JA: **Is the 5-HT(7) receptor involved in the pathogenesis and prophylactic treatment of migraine?** *Eur J Pharmacol* 2002, **439:**1-11.

42. Baker LP, Nielsen MD, Impey S, Metcalf MA, Poser SW, Chan G, Obrietan K, Hamblin MW, Storm DR: **Stimulation of type 1 and type 8 Ca2+/calmodulin-sensitive adenylyl cyclases by the Gs-coupled 5-hydroxytryptamine subtype 5-HT7A receptor.** *J Biol Chem* 1998, **273:**17469-17476.

43. Hamblin MW, Guthrie CR, Kohen R, Heidmann DE: **Gs protein-coupled serotonin receptors: receptor isoforms and functional differences.** *Ann N Y Acad Sci* 1998, **861:**31-37.

44. Ohta T, Ikemi Y, Murakami M, Imagawa T, Otsuguro K, Ito S: **Potentiation of transient receptor potential V1 functions by the activation of metabotropic 5-HT receptors in rat primary sensory neurons.** *J Physiol* 2006, **576:**809-822.

45. Cho SY, Ki HG, Kim JM, Oh JM, Yang JH, Kim WM, Lee HG, Yoon MH, Choi JI: **Expression of the spinal 5-HT7 receptor and p-ERK pathway in the carrageenan inflammatory pain of rats.** *Korean J Anesthesiol* 2015, **68:**170-174.

46. Wang X, Fang Y, Liang J, Yin Z, Miao J, Luo N: **Selective inhibition of 5-HT7 receptor reduces CGRP release in an experimental model for migraine.** *Headache* 2010, **50:**579-587.

47. Zimmermann M: **Ethical guidelines for investigations of experimental pain in conscious animals.** *Pain* 1983, **16:**109-110.

48. Boyer N, Dallel R, Artola A, Monconduit L: **General trigeminospinal central sensitization and impaired descending pain inhibitory controls contribute to migraine progression.** *Pain* 2014, **155:**1196-1205.

49. Bishop J, Becerra L, Barmettler G, Chang P-C, Kainz V, Burstein R, Borsook D: **Modulation of brain networks by sumatriptan-naproxen in the inflammatory soup migraine model.** *PAIN* 2019, **160:**2161-2171.

50. Lapirot O, Chebbi R, Monconduit L, Artola A, Dallel R, Luccarini P: **NK1 receptor-expressing spinoparabrachial neurons trigger diffuse noxious inhibitory controls through lateral parabrachial activation in the male rat.** *Pain* 2009, **142:**245-254.

51. Hoffman MS, Mitchell GS: **Spinal 5-HT7 receptor activation induces long-lasting phrenic motor facilitation.** *The Journal of Physiology* 2011, **589:**1397-1407.

52. Ni J, Cao N, Wang X, Zhan C, Si J, Gu B, Andersson K-E: **The serotonin (5-hydroxytryptamine) 5-HT7 receptor is up-regulated in Onuf's nucleus in rats with chronic spinal cord injury.** *BJU International* 2019, **123:**718-725.

53. Wang XR, Yang JW, Ji CS, Zeng XH, Shi GX, Fisher M, Liu CZ: **Inhibition of NADPH Oxidase-Dependent Oxidative Stress in the Rostral Ventrolateral Medulla Mediates the Antihypertensive Effects of Acupuncture in Spontaneously Hypertensive Rats.** *Hypertension* 2018, **71:**356-365.

54. Xu X, Liu L, Zhao L, Li B, Jing X, Qu Z, Zhu Y, Zhang Y, Li Z, Fisher M, et al: **Effect of Electroacupuncture on Hyperalgesia and Vasoactive Neurotransmitters in a Rat Model of Conscious Recurrent Migraine.** *Evidence-Based Complementary and Alternative Medicine* 2019, **2019:**1-14.

55. Zhang CH, Bian JL, Meng ZH, Meng LN, Ren XS, Wang ZL, Guo XY, Shi XM: **Tongguan Liqiao acupuncture therapy improves dysphagia after brainstem stroke.** *Neural Regen Res* 2016, **11:**285-291.

56. Zhao L, Liu L, Xu X, Qu Z, Zhu Y, Li Z, Zhao J, Wang L, Jing X, Li B: **Electroacupuncture Inhibits Hyperalgesia by Alleviating Inflammatory Factors in a Rat Model of Migraine.** *J Pain Res* 2020, **13:**75-86.

57. Fregni F, Macedo IC, Spezia-Adachi LN, Scarabelot VL, Laste G, Souza A, Sanches PRS, Caumo W, Torres ILS: **Transcranial direct current stimulation (tDCS) prevents chronic stress-induced hyperalgesia in rats.** *Brain Stimulation* 2018, **11:**299-301.

58. Dixon WJ: **Efficient analysis of experimental observations.** *Annu Rev Pharmacol Toxicol* 1980, **20:**441-462.

59. Chaplan SR, Bach FW, Pogrel JW, Chung JM, Yaksh TL: **Quantitative assessment of tactile allodynia in the rat paw.** *Journal of Neuroscience Methods* 1994, **53:**55-63.

60. Lopez-Canul M, Palazzo E, Dominguez-Lopez S, Luongo L, Lacoste B, Comai S, Angeloni D, Fraschini F, Boccella S, Spadoni G, et al: **Selective melatonin MT2 receptor ligands relieve neuropathic pain through modulation of brainstem descending antinociceptive pathways.** *PAIN* 2015, **156:**305-317.

61. Yadlapalli JSK, Ford BM, Ketkar A, Wan A, Penthala NR, Eoff RL, Prather PL, Dobretsov M, Crooks PA: **Antinociceptive effects of the 6- O -sulfate ester of morphine in normal and diabetic rats: Comparative role of mu- and delta-opioid receptors.** *Pharmacological Research* 2016, **113:**335-347.

62. Kooshki R, Abbasnejad M, Esmaeili-Mahani S, Raoof M, Sheibani V: **Activation orexin 1 receptors in the ventrolateral periaqueductal gray matter attenuate nitroglycerin-induced migraine attacks and calcitonin gene related peptide up-regulation in trigeminal nucleus caudalis of rats.** *Neuropharmacology* 2020:107981.

63. Lopes BC, Medeiros LF, Silva De Souza V, Cioato SG, Medeiros HR, Regner GG, Lino De Oliveira C, Fregni F, Caumo W, Torres ILS: **Transcranial direct current stimulation combined with exercise modulates the inflammatory profile and hyperalgesic response in rats subjected to a neuropathic pain model: Long-term effects.** *Brain Stimulation* 2020, **13:**774-782.

64. Jasmin L, Kohan L, Franssen M, Janni G, Goff JR: **The cold plate as a test of nociceptive behaviors: description and application to the study of chronic neuropathic and inflammatory pain models.** *Pain* 1998, **75:**367-382.

65. Gong K, Jasmin L: **Sustained Morphine Administration Induces TRPM8-Dependent Cold Hyperalgesia.** *J Pain* 2017, **18:**212-221.

66. Hu JW: **Response properties of nociceptive and non-nociceptive neurons in the rat's trigeminal subnucleus caudalis (medullary dorsal horn) related to cutaneous and deep craniofacial afferent stimulation and modulation by diffuse noxious inhibitory controls.** *Pain* 1990, **41:**331-345.

67. Burstein R, Yamamura H, Malick A, Strassman AM: **Chemical stimulation of the intracranial dura induces enhanced responses to facial stimulation in brain stem trigeminal neurons.** *J Neurophysiol* 1998, **79:**964-982.

68. Wang S, Wang J, Liu K, Bai W, Cui X, Han S, Gao X, Zhu B: **Signaling Interaction between Facial and Meningeal Inputs of the Trigeminal System Mediates Peripheral Neurostimulation Analgesia in a Rat Model of Migraine.** *Neuroscience* 2020, **433:**184-199.

69. Raboisson P, Dallel R, Clavelou P, Sessle BJ, Woda A: **Effects of subcutaneous formalin on the activity of trigeminal brain stem nociceptive neurones in the rat.** *J Neurophysiol* 1995, **73:**496-505.

70. Mitsikostas DD, Knight YE, Lasalandra M, Kavantzas N, Goadsby PJ: **Triptans attenuate capsaicin-induced CREB phosphorylation within the trigeminal nucleus caudalis: a mechanism to prevent central sensitization?** *J Headache Pain* 2011, **12:**411-417.

71. Zanassi P, Paolillo M, Feliciello A, Avvedimento EV, Gallo V, Schinelli S: **cAMP-dependent protein kinase induces cAMP-response element-binding protein phosphorylation via an intracellular calcium release/ERK-dependent pathway in striatal neurons.** *J Biol Chem* 2001, **276:**11487-11495.

72. Skalhegg BS, Tasken K: **Specificity in the cAMP/PKA signaling pathway. Differential expression,regulation, and subcellular localization of subunits of PKA.** *Front Biosci* 2000, **5:**D678-693.

73. Han JS: **Acupuncture: neuropeptide release produced by electrical stimulation of different frequencies.** *Trends Neurosci* 2003, **26:**17-22.

74. Su TF, Zhang LH, Peng M, Wu CH, Pan W, Tian B, Shi J, Pan HL, Li M: **Cannabinoid CB2 receptors contribute to upregulation of β-endorphin in inflamed skin tissues by electroacupuncture.** *Mol Pain* 2011, **7:**98.

75. Goldman N, Chen M, Fujita T, Xu Q, Peng W, Liu W, Jensen TK, Pei Y, Wang F, Han X, et al: **Adenosine A1 receptors mediate local anti-nociceptive effects of acupuncture.** *Nat Neurosci* 2010, **13:**883-888.

76. Gu J, Luo L, Wang Q, Yan S, Lin J, Li D, Cao B, Mei H, Ying B, Bin L, et al: **Maresin 1 attenuates mitochondrial dysfunction through the ALX/cAMP/ROS pathway in the cecal ligation and puncture mouse model and sepsis patients.** *Lab Invest* 2018, **98:**715-733.

77. Wang J, Wu M, Lin X, Li Y, Fu Z: **Low-Concentration Oxygen/Ozone Treatment Attenuated Radiculitis and Mechanical Allodynia via PDE2A-cAMP/cGMP-NF-κB/p65 Signaling in Chronic Radiculitis Rats.** *Pain Res Manag* 2018, **2018:**5192814.

78. Miyano K, Shiraishi S, Minami K, Sudo Y, Suzuki M, Yokoyama T, Terawaki K, Nonaka M, Murata H, Higami Y, Uezono Y: **Carboplatin Enhances the Activity of Human Transient Receptor Potential Ankyrin 1 through the Cyclic AMP-Protein Kinase A-A-Kinase Anchoring Protein (AKAP) Pathways.** *Int J Mol Sci* 2019, **20.**

79. Ye Y, Li H, Yang JW, Wang XR, Shi GX, Yan CQ, Ma SM, Zhu W, Li QQ, Li TR, et al: **Acupuncture Attenuated Vascular Dementia-Induced Hippocampal Long-Term Potentiation Impairments via Activation of D1/D5 Receptors.** *Stroke* 2017, **48:**1044-1051.

80. Cui WQ, Sun WS, Xu F, Hu XM, Yang W, Zhou Y, Du LX, Zhang WW, Mao-Ying QL, Mi WL, et al: **Spinal Serotonin 1A Receptor Contributes to the Analgesia of Acupoint Catgut Embedding by Inhibiting Phosphorylation of the N-Methyl-d-Aspartate Receptor GluN1 Subunit in Complete Freund's Adjuvant-Induced Inflammatory Pain in Rats.** *J Pain* 2019, **20:**16 e11-16 e16.

81. Ji RR: **Peripheral and central mechanisms of inflammatory pain, with emphasis on MAP kinases.** *Curr Drug Targets Inflamm Allergy* 2004, **3:**299-303.
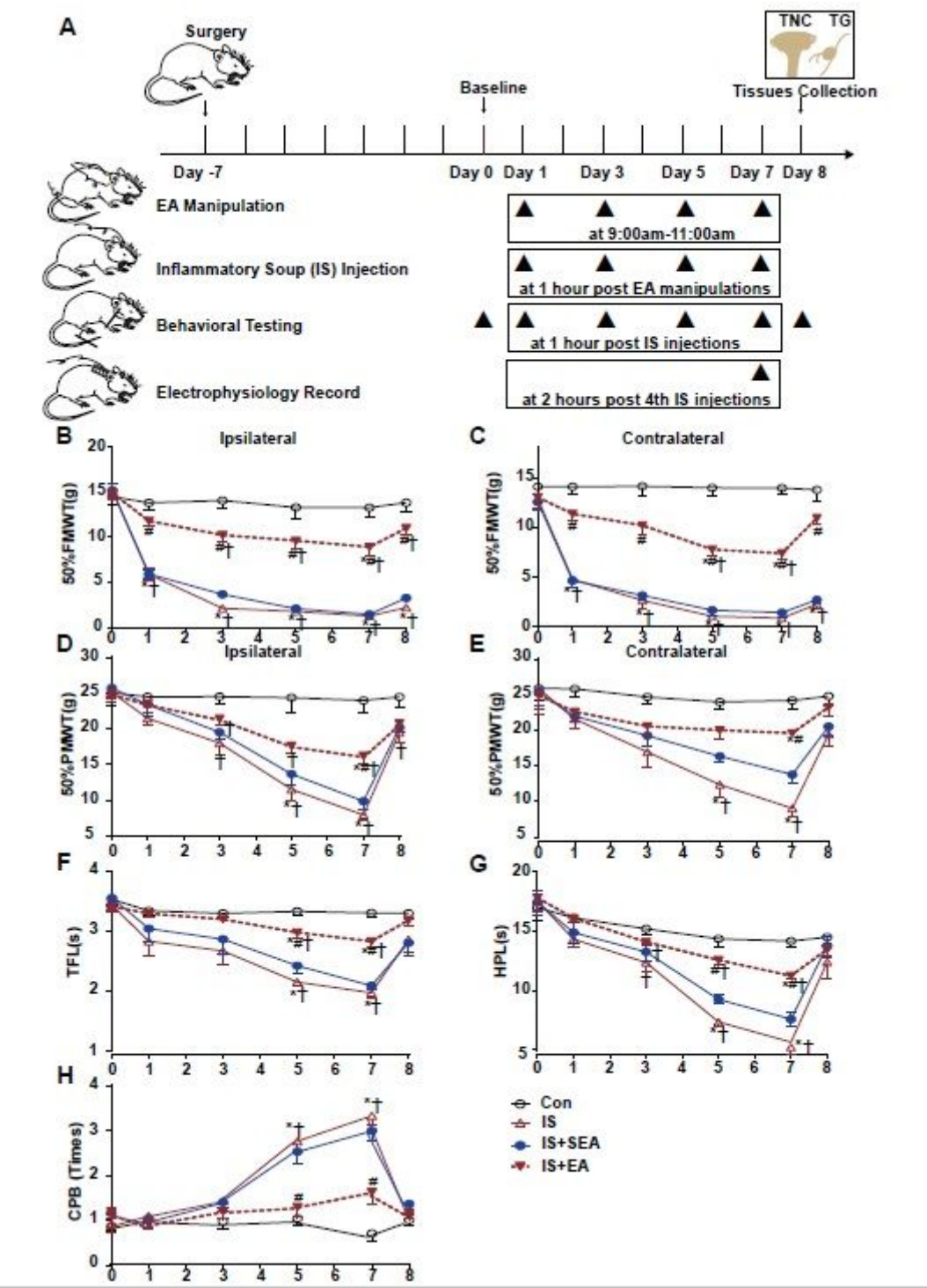
Figures

Figure 1

Effects of EA on IS-induced mechanical and thermal hyperalgesia. (A) Scheme of the experimental design. Rats were applied EA manipulation, following repeated-dural IS injection at day 1, day 3, day 5, day 7, then measurements of 50%FMWT, 50%PMWT, TFL, HPL, and CPB to examine the extent of mechanical and thermal hyperalgesia after 1 hours of IS injection, and also the day 0 without IS injection

and one day after 4th IS injection (day8). (B and C) Reduction in 50%FMWT of IS+EA and IS compared with the Con group (n = 10; *P < 0. 05); increase in 50%FMWT of IS+EA compared with the IS group on the bilateral side (n = 10; #P < 0.05). (D and E) Effects of EA on extracephalic mechanical hyperalgesia after dural IS injection. There was an increase of the 50%PMWT in the IS+EA group compared with the IS group on the bilateral side (n = 10, #P < 0.05). The TFL (F), HPL (G) decrease and CPB (H) increase in the IS group compared with the Con group(n = 10, *P < 0.05) at day5 and day 7, there was an increase of the TFL, HPL and a decrease of CPB in the IS+EA compared with the in the IS group (n = 10, #P < 0.05). The repeated-measure 2-way ANOVA post hoc Turkey multiple comparison test was used. Group values are indicated by mean ± SEM. *P < 0.05 compared with the IS group, #P < 0.05 compared with the IS+EA group at the same time point; †P < 0.05 compared with the baseline at day 0. 50%FMWT, 50% facial mechanical withdrawal threshold; 50%PMWT, 50% paw mechanical withdrawal threshold; TFL, tail-flick latency; HPL, hot-plate latency; CPB, cold-plate behaviors; EA, electroacupuncture; IS, inflammatory soup; SEA, sham electroacupuncture; Con, control.
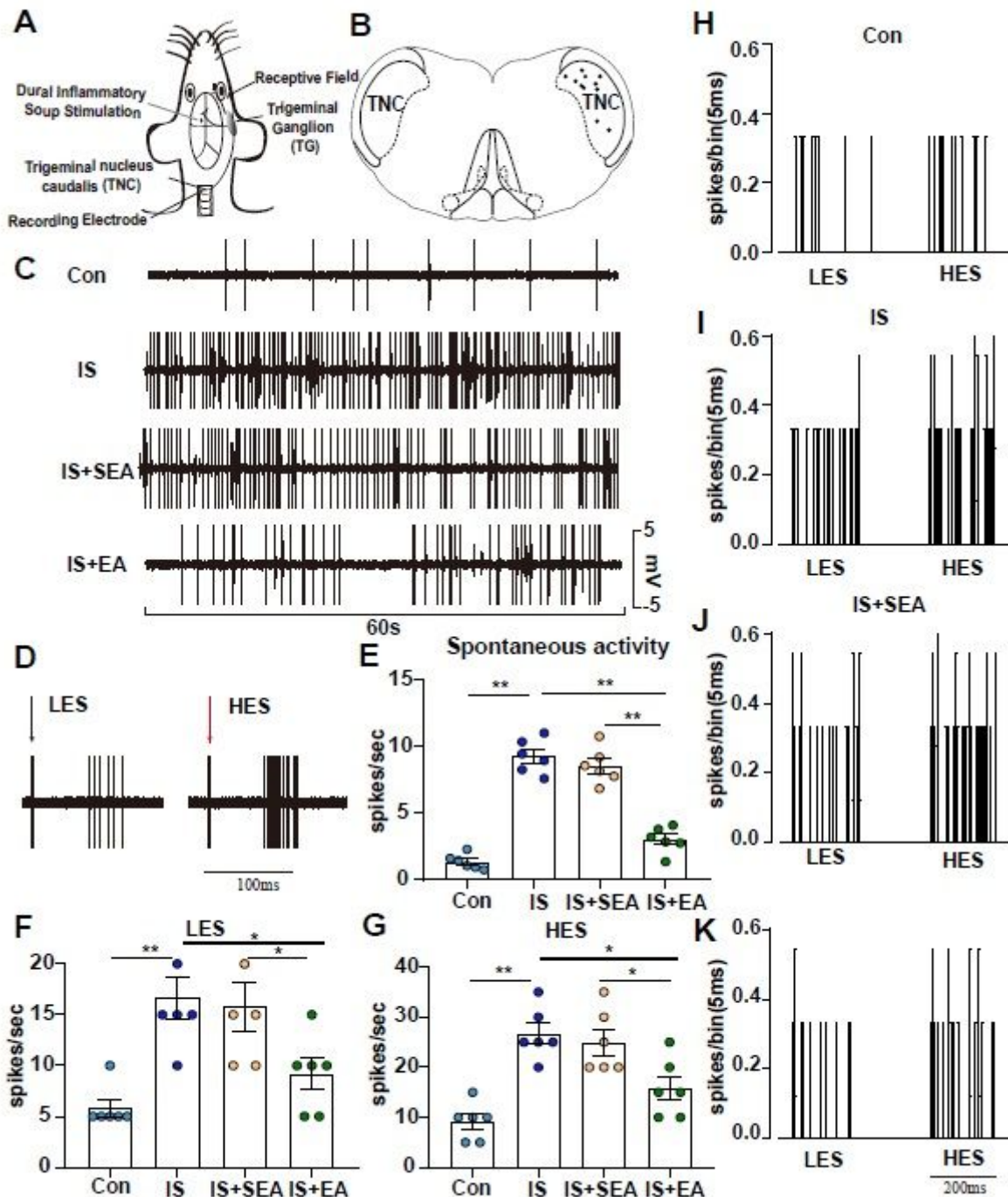
Figure 2

Overview of the electrophysiological recordings and neuronal characteristics among the Con, IS, IS+SEA, IS+EA groups. (A) Experimental setup with percutaneous electrical stimulation and recording of neurons in the TNC. (B) The location of recording sites in the TNC from which recordings of nociceptive neurons, receiving convergent input from the dura mater and facial receptive field, were made. The locations were reconstructed from lesions (•) and are located in laminae Ⅰ-Ⅱ. (C) Spontaneous activity was recorded for 60 seconds at 30 minutes post-finding the activated neurons for stabilization among the indicated groups. (D) An original tracing from a typical unit (second-order neurons) responding to percutaneous

electrical stimulation in low (1Tc (2mA), LES) and high (2.5Tc (5mA), HES) intensity (latencies in the C-fiber range). Black arrow represents stimulus artifact. spontaneous activity (E), LES-evoked responses (F) and HES-evoked responses (G) of WDR neurons recorded 2 hours after the 4th IS or aCSF injection in the TCC of none manipulation (Con and IS) (H and I), SEA (IS+SEA) (J) or EA (IS+EA) (K) rats. Note that, compared with SEA-treated rats, all these aspects of central sensitization are strongly reduced in EA-treated ones, consistent with the conclusion that EA treatment prevents neuronal sensitization within the TNC. When four groups were compared for Electrophysiology, a Kruskal-Wallis test was used, and when only two groups were compared, a Mann-Whitney test was used. Group values are indicated by mean ± SEM. *P < 0.05, **P < 0.01. Tc: the stimulation intensities required to evoke neuronal activity with a conductive velocity of 0.4-2 m.s-1, namely about 2mA. LES, low intensity electrostimulation; HES, high intensity electrostimulation; WDR, Wide-dynamic range; TG, trigeminal ganglion; TNC, trigeminal nucleus caudalis; EA, electroacupuncture; IS, inflammatory soup; aCSF, artificial cerebrospinal fluid; SEA, sham electroacupuncture; Con, control.
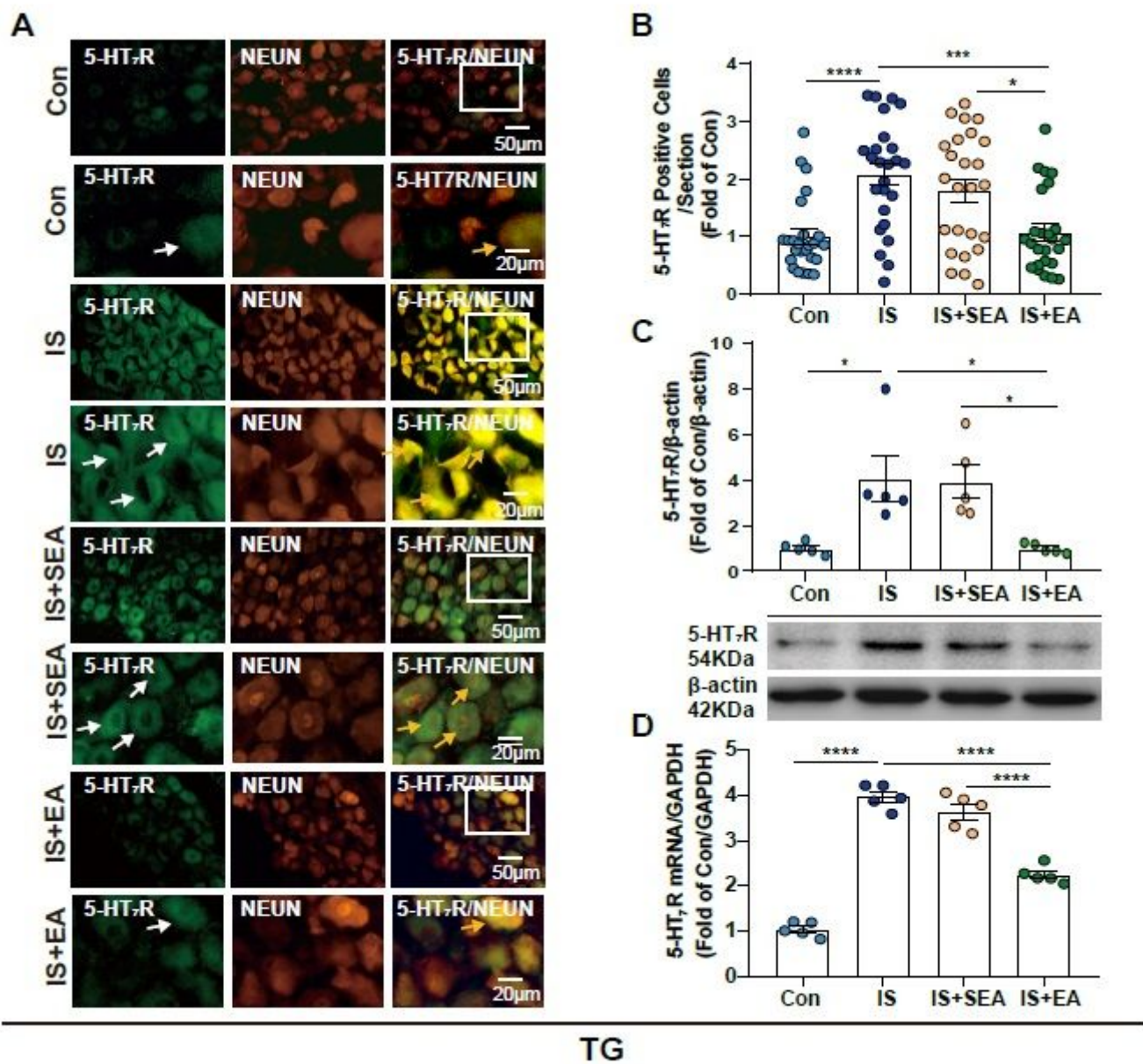
Figure 3

Effects of EA on the formation of endogenous 5-HT7R in the TG at day 8 after 4th IS injection. (A) Immunohistochemical staining showed that 5-HT7R (green) were expressed mostly in the individual neurons (NeuN, Neuron marker, red) of the TG. The upper panel displays the expression of 5-HT7R at low magnification, and the lower panel displays the expression of 5-HT7R in the TG at high magnification in each group. The white and orange arrow points to the positive cells in TG. Scale bars = 50 μm or 20 μm. (B) EA caused a decrease in endogenous 5-HT7R expression on the ipsilateral side in TG. Quantitative analyses of 5-HT7R to evaluate the numbers of positive cells (n = 5, 5 sections/animal). (C) Representative western blot bands and quantitative analyses of 5-HT7R. The same membranes were probed for 5-HT7R with β-actin. (n = 5). (D) The mRNA levels of 5-HT7R were also accessed by real-time polymerase chain reaction, and values were corrected by GAPDH in TG (n = 5). One-way ANOVA followed by post hoc Tukey test. Group values are indicated by mean ± SEM. $*P < 0.05$, $**P < 0.01$, $***P < 0.001$, $****P < 0.0001$. 5-HT7R, 5-hydroxytryptamine (5-HT)7 receptor; GAPDH, glycolytic enzyme glyceraldehyde 3-phosphate dehydrogenase; TG, trigeminal ganglion; EA, electroacupuncture; IS, inflammatory soup; SEA, sham electroacupuncture; Con, control.
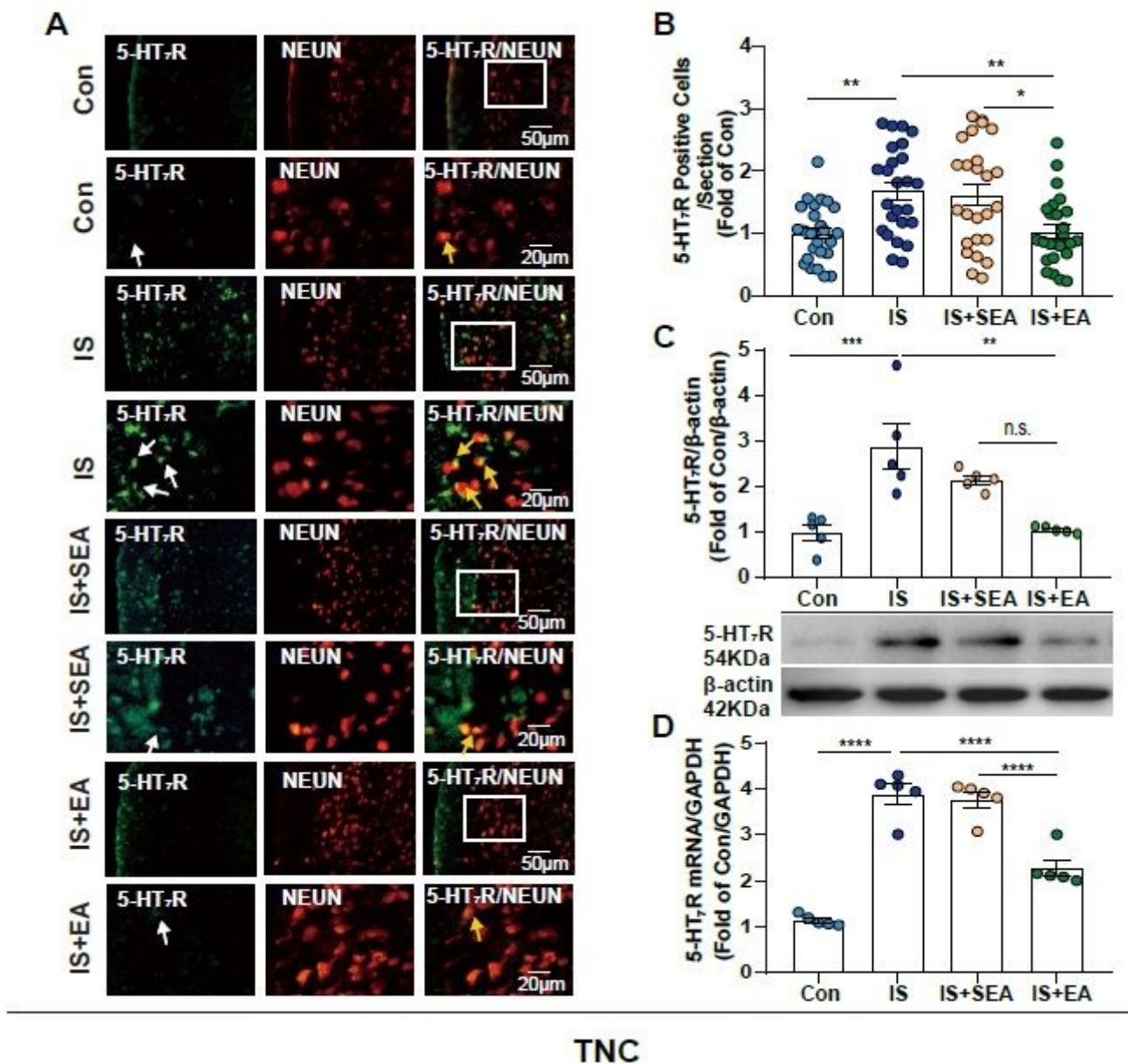
Figure 4

Effects of EA on the formation of endogenous 5-HT7R in the TNC at day 8 after 4th IS injection. (A) Immunohistochemical staining showed that 5-HT7R (green) were expressed mostly in the individual neurons (NeuN, Neuron marker, red) of the TNC. The upper panel displays the expression of 5-HT7R at low magnification, and the lower panel displays the expression of 5-HT7R in the TNC at high magnification in each group. The white and orange arrow points to the positive cells in TNC. Scale bars = 50 μm or 20 μm. (B) EA caused a decrease in endogenous 5-HT7R expression on the ipsilateral side in TNC. Quantitative analyses of 5-HT7R to evaluate the numbers of positive cells (n = 5, 5 sections/animal). (C) Representative western blot bands and quantitative analyses of 5-HT7R. The same membranes were probed for 5-HT7R with β-actin. (n = 5). (D) The mRNA levels of 5-HT7R were also accessed by real-time polymerase chain reaction, and values were corrected by GAPDH in TNC (n = 5).

One-way ANOVA followed by post hoc Tukey test. Group values are indicated by mean ± SEM. *P < 0.05, **P < 0.01, ***P < 0.001, ****P < 0.0001. 5-HT7R, 5-hydroxytryptamine (5-HT)7 receptor; TNC, trigeminal nucleus caudalis; EA, electroacupuncture; IS, inflammatory soup; SEA, sham electroacupuncture; Con, control.
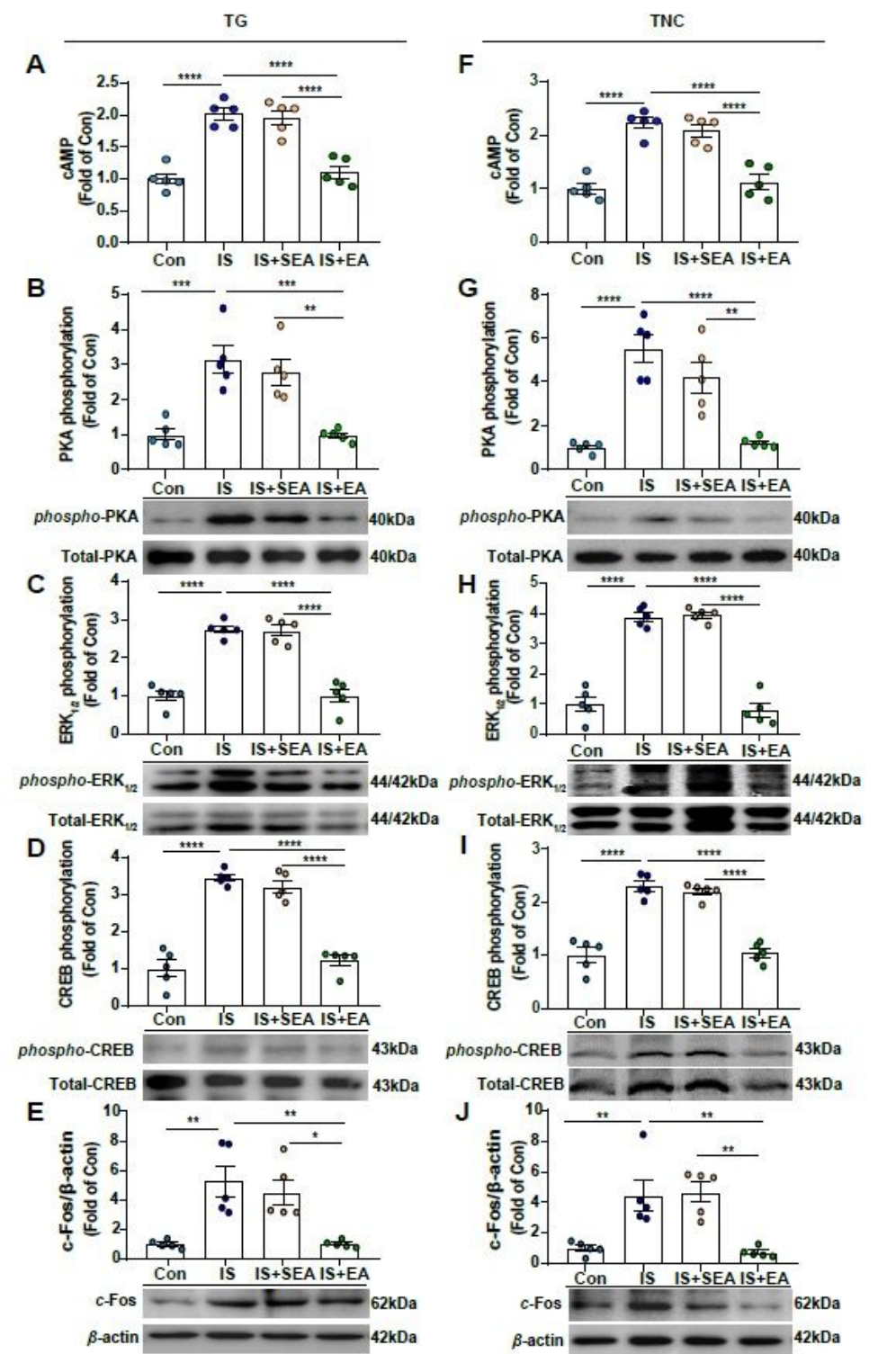

Figure 5

Effects of EA on the protein levels of cAMP and 5-HT7R-mediated PKA, ERK1/2 phosphorylation signaling pathway in dural 4th IS injection rats. The cAMP content decreased in the IS+EA group compared with the IS group on the ipsilateral side (n = 5) (A and F). Representative Western blots of phosphorylated and total PKA (B and G), ERK1/2 (extracellular signal-regulated protein kinase1/2) (C and H), and CREB (D and I), as well as c-Fos (E and J). The densitometric analysis of phosphorylated and c-Fos protein levels detected from the TG and TNC of Con, IS, IS+SEA, IS+EA. One-way ANOVA followed by post hoc Tukey test. Group values are indicated by mean ± SEM. *$P < 0.05$, **$P < 0.01$, ***$P < 0.001$, ****$P < 0.0001$. 5-HT7R, 5-hydroxytryptamine (5-HT)7 receptor; cAMP, cyclic adenosine monophosphate; PKA, protein kinase A; ERK1/2, extracellular signal-regulated kinase1/2; CREB, cAMP responsive element-binding protein. TNC, trigeminal nucleus caudalis; TG, trigeminal ganglion; EA, electroacupuncture; IS, inflammatory soup; SEA, sham electroacupuncture; Con, control.
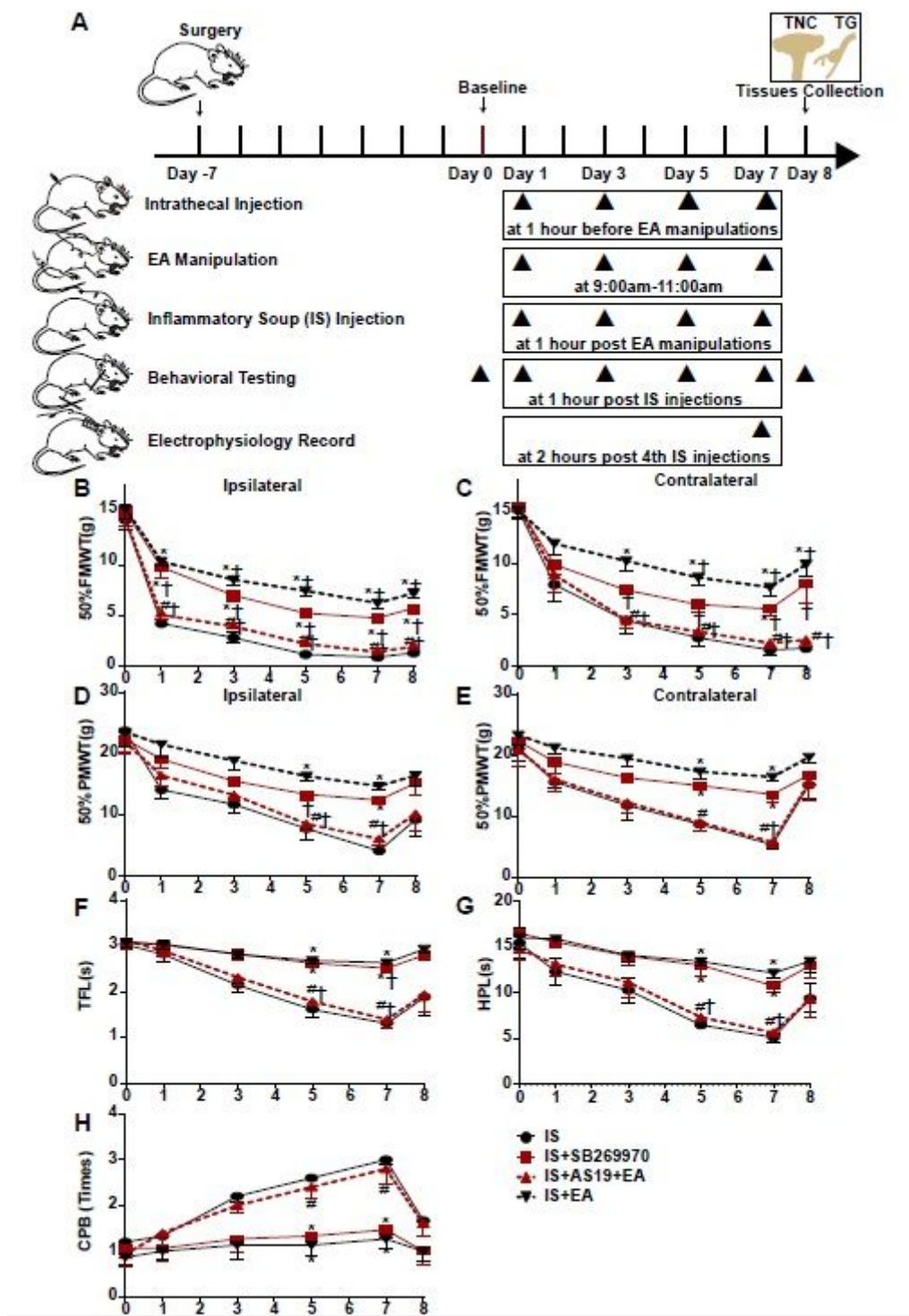
Figure 6

Injecting 5-HT7R agonist AS19 and 5-HT7R antagonist SB269970 into the intrathecal space of IS rats, evaluate the antihyperalgesic effects of EA and SB269970 in IS rats. (A) Scheme of the experimental design. Rats were injected 5-HT7R agonist AS19 and 5-HT7R antagonist SB269970 into the intrathecal space, following EA manipulation application and repeated-dural IS injection at day 1, day 3, day 5, day 7, then measurements of 50%FMWT, 50%PMWT, TFL, HPL, and CPB to examine the extent of mechanical and thermal hyperalgesia after 1 hours of IS injection, and aslo the day 0 without IS injection and one day after 4th IS injection (day8). Changes in mechanical (50% FMWT (B and C), and 50% PMWT (D and E))

and thermal (TFL (F), HPL (G), and CPB (H)) hyperalgesia in IS, IS+SB269970, IS+AS19+EA, IS+EA group at day0, day1, day3, day5, day7, day8 (n = 5). The repeated-measure 2-way ANOVA post hoc Turkey multiple comparison test was used. Group values are indicated by mean ± SEM. *$P < 0.05$ compared with the IS group, #$P < 0.05$ compared with the IS+EA group at the same time point. †$P < 0.05$ compared with the baseline at day 0. 5-HT7R, 5-hydroxytryptamine (5-HT)7 receptor; 50%FMWT, 50% facial mechanical withdrawal threshold; 50%PMWT, 50% paw mechanical withdrawal threshold; TFL, tail-flick latency; HPL, hot-plate latency; CPB, cold-plate behaviors; EA, electroacupuncture; IS, inflammatory soup; AS19, 5-HT7R agonist; SB269970, 5-HT7R antagonist.
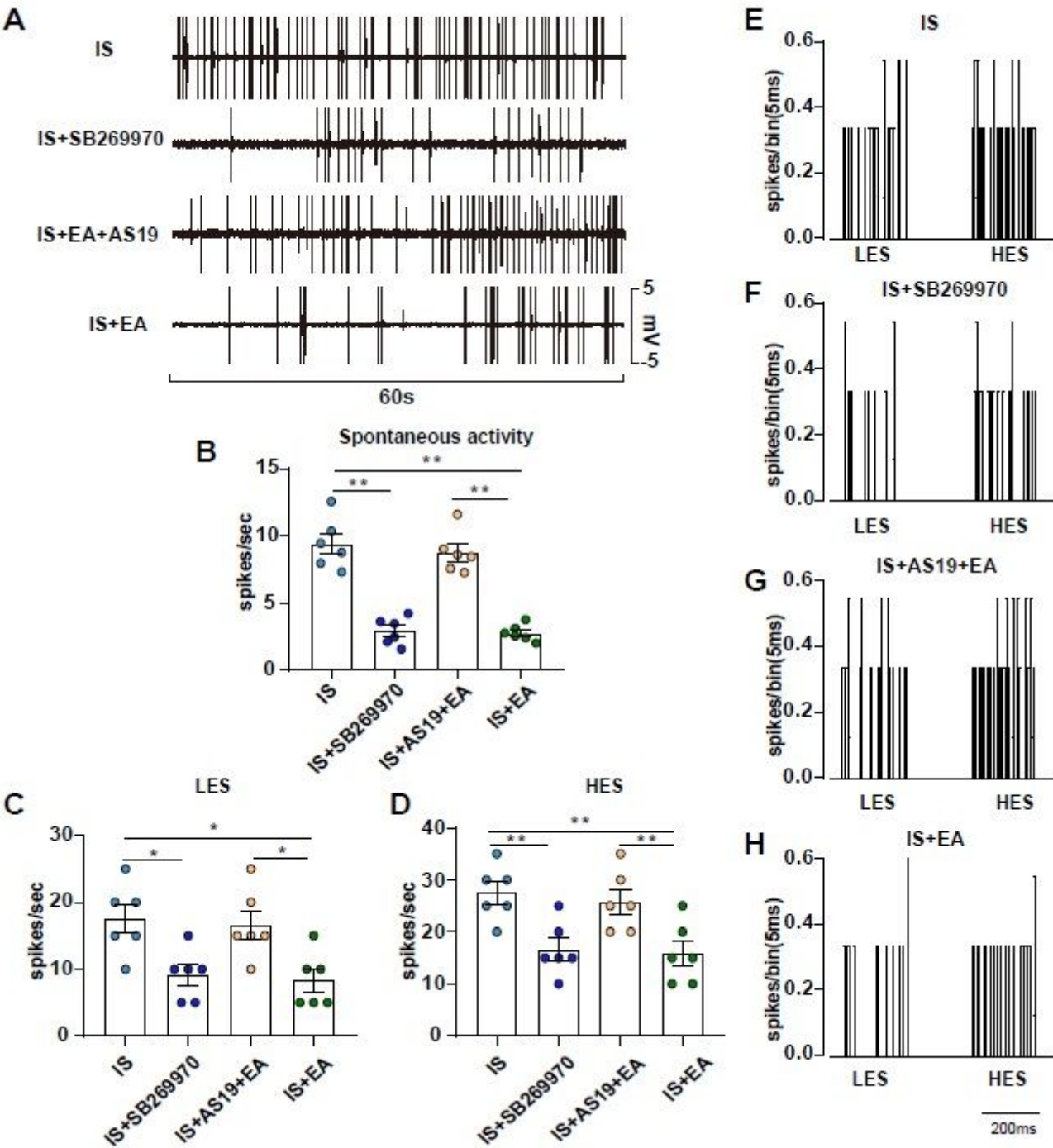

Figure 7

Overview of the electrophysiological recordings and neuronal characteristics among the IS, IS+SB269970, IS+AS19+EA, IS+EA groups. (A) Spontaneous activity was recorded for 60 seconds at 30 minutes post-finding the activated neurons for stabilization among the indicated groups. Spontaneous activity (B), LES-evoked responses (C) and HES-evoked responses (D) of WDR neurons recorded 2 hours after the 4th IS or aCSF injection in the TCC of none manipulation (IS and IS+SB269970) (E and F), EA (IS+AS19+EA and IS+EA) (G and H) rats. Note that, compared with IS rats, all these aspects of central sensitization are strongly reduced in EA- and SB267790-treated ones, consistent with the conclusion that 5-HT7R antagonist mimicked EA treatment prevents neuronal sensitization within the TNC. When four groups were compared for Electrophysiology, a Kruskal-Wallis test was used, and when only two groups were compared, a Mann-Whitney test was used. Group values are indicated by mean ± SEM. *$P < 0.05$, **$P < 0.01$. Tc: the stimulation intensities required to evoke neuronal activity with a conductive velocity of 0.4-2 m.s-1, namely about 2mA. 5-HT7R, 5-hydroxytryptamine (5-HT)7 receptor; LES, low intensity electrostimulation; HES, high intensity electrostimulation; WDR, Wide-dynamic range; TNC, trigeminal nucleus caudalis; aCSF, artificial cerebrospinal fluid; EA, electroacupuncture; IS, inflammatory soup; AS19, 5-HT7R agonist; SB269970, 5-HT7R antagonist.
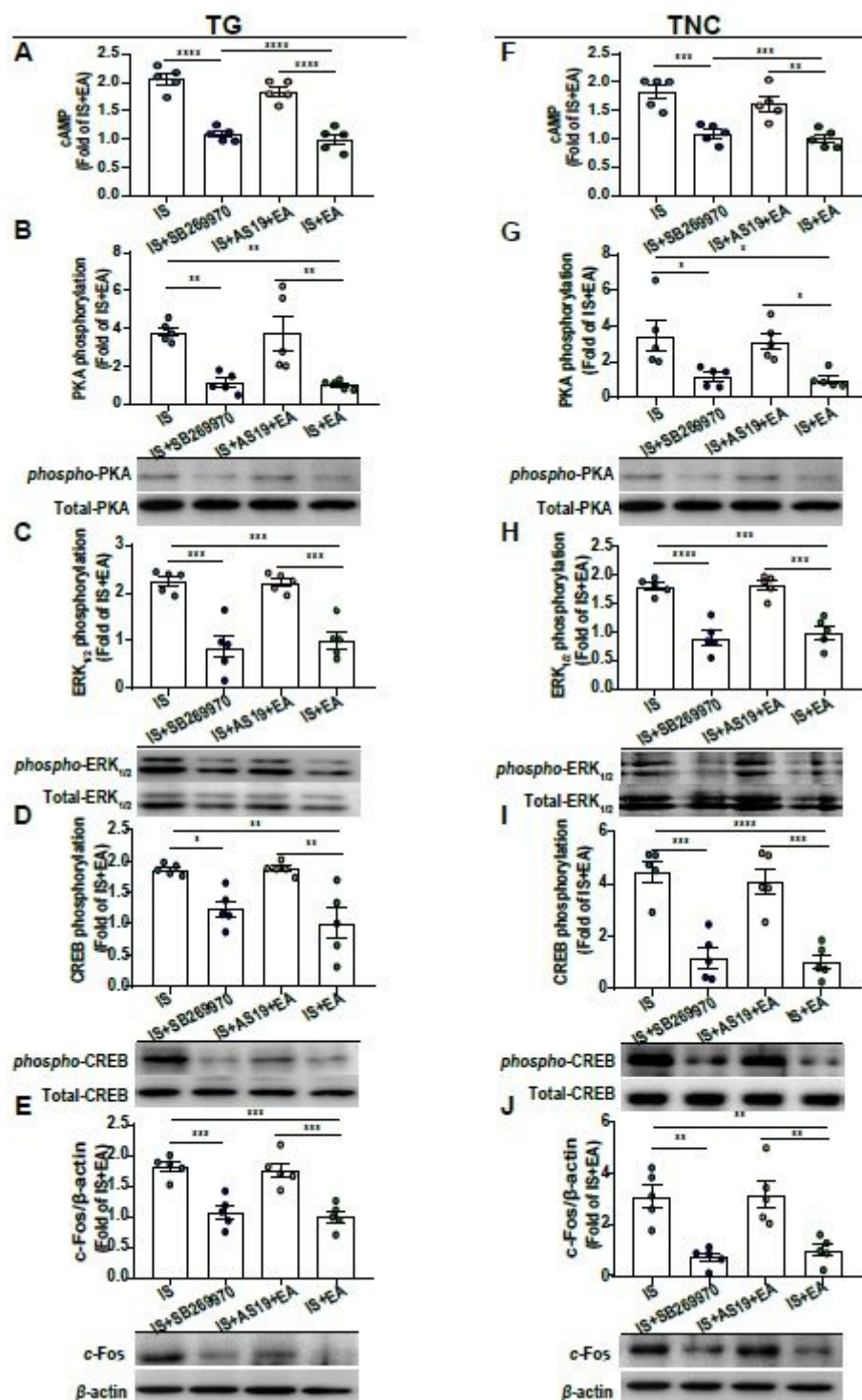
Figure 8

Effects of 5-HT7R on the protein levels of cAMP and 5-HT7R-mediated PKA, ERK1/2 phosphorylation signaling pathway in IS and IS+EA rats. The cAMP content decreased in the IS+EA and IS+SB269970 group compared with the IS group on the ipsilateral side (n = 5) (A and F). Representative Western blots of phosphorylated and total PKA (B and G), ERK1/2 (C and H), and CREB (D and I), as well as c-Fos (E and J). (A and J) The densitometric analysis of phosphorylated and c-Fos protein levels detected from the TG and TNC of IS, IS+SB269970, IS+AS19+EA, IS+EA. One-way ANOVA followed by post hoc Tukey test. Group values are indicated by mean ± SEM. *$P < 0.05$, **$P < 0.01$, ***$P < 0.001$, ****$P < 0.001$. 5-

HT7R, 5-hydroxytryptamine (5-HT)7 receptor; PKA, protein kinase A; ERK1/2, extracellular signal-regulated kinase1/2; CREB, cAMP responsive element-binding protein; TG, trigeminal ganglion; TNC, trigeminal nucleus caudalis; EA, electroacupuncture; IS, inflammatory soup; AS19, 5-HT7R agonist; SB269970, 5-HT7R antagonist.
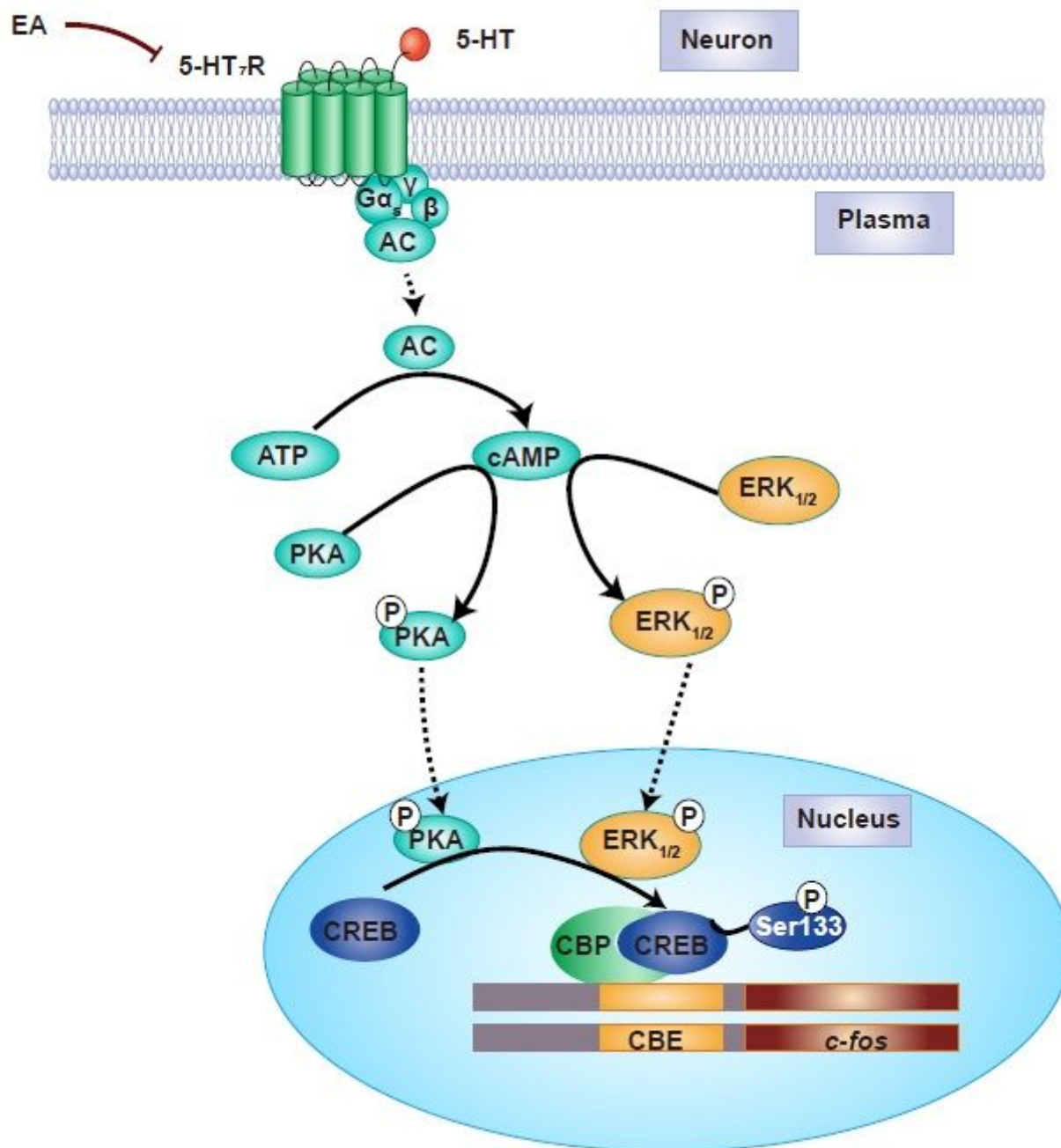

Figure 9

Proposed mechanism of the antihyperalgesic effects of EA stimulation. Before EA, there is a relatively high amount of 5-HT7R protein in TG and TNC of IS rats. The medial cAMP is formulated in the cytoplasm of neuron, resulting in PKA and ERK1/2 phosphorylation. Once PKA and ERK1/2 is phosphorylated into p-PKA and p-ERK1/2, the CREB will move from the cytoplasm into the nuclear, and phosphorylated at Ser133. Following nuclear CREB-CBP elevation, the initiate or potentiate of early gene c-fos was regulated by p-CREB-mediated transcription, resulting in dural IS stimulation that leads to hyperalgesia. By contrast, EA treatment decreases the amount of 5-HT7R proteins, forming lower cAMP, thereby PKA and ERK1/2 phosphorylation is inhibited in the cytoplasm. This prevents CREB phosphorylation, and therefore gene c-fos silence, ultimately producing an antihyperalgesic effect. 5-HT7R, 5-hydroxytryptamine (5-HT)7 receptor; cAMP, cyclic adenosine monophosphate; PKA, protein kinase A; ERK1/2, extracellular signal-regulated kinase1/2; CREB, cAMP responsive element-binding protein; EA, electroacupuncture.

Supplementary Files

This is a list of supplementary files associated with this preprint. Click to download.

- Additionalfile.pdf